



THE UNIVERSITY *of* EDINBURGH

## Edinburgh Research Explorer

### CyanoGate

**Citation for published version:**

Vasudevan, R, Gale, G, Schiavon osorio, AA, Puzorjov, A, Malin, J, Gillespie, MD, Vavitsas, K, Zulkower, V, Wang, B, Howe, CJ, Lea-Smith, DJ & McCormick, A 2019, 'CyanoGate: A modular cloning suite for engineering cyanobacteria based on the plant MoClo syntax', *Plant physiology*, vol. 180, no. 1, pp. 39-55. <https://doi.org/10.1104/pp.18.01401>

**Digital Object Identifier (DOI):**

[10.1104/pp.18.01401](https://doi.org/10.1104/pp.18.01401)

**Link:**

[Link to publication record in Edinburgh Research Explorer](#)

**Document Version:**

Peer reviewed version

**Published In:**

Plant physiology

**Publisher Rights Statement:**

Copyright © 2019 American Society of Plant Biologists. All rights reserved.  
Copyright 2019 by the American Society of Plant Biologists.

**General rights**

Copyright for the publications made accessible via the Edinburgh Research Explorer is retained by the author(s) and / or other copyright owners and it is a condition of accessing these publications that users recognise and abide by the legal requirements associated with these rights.

**Take down policy**

The University of Edinburgh has made every reasonable effort to ensure that Edinburgh Research Explorer content complies with UK legislation. If you believe that the public display of this file breaches copyright please contact [openaccess@ed.ac.uk](mailto:openaccess@ed.ac.uk) providing details, and we will remove access to the work immediately and investigate your claim.



1 *Short Title:* A Golden Gate-based toolkit for cyanobacteria

2

3 *Corresponding author:* Alistair McCormick, School of Biological Sciences, University of  
4 Edinburgh, +44 (0)1316505316, alistair.mccormick@ed.ac.uk

5

6 ***Title:* CyanoGate: A modular cloning suite for engineering cyanobacteria based on the  
7 plant MoClo syntax**

8

9 *Authors:* Ravendran Vasudevan<sup>1,2</sup>, Grant A.R. Gale<sup>1,2,3</sup>, Alejandra A. Schiavon<sup>1,2</sup>, Anton  
10 Puzorjov<sup>1,2</sup>, John Malin<sup>1,2</sup>, Michael D. Gillespie<sup>4</sup>, Konstantinos Vavitsas<sup>5,6</sup>, Valentin  
11 Zulkower<sup>2</sup>, Baojun Wang<sup>2,3</sup>, Christopher J. Howe<sup>7</sup>, David J. Lea-Smith<sup>4</sup>, Alistair J.  
12 McCormick\*<sup>1,2</sup>

13

14 <sup>1</sup>Institute of Molecular Plant Sciences, School of Biological Sciences, University of Edinburgh,  
15 EH9 3BF, UK.

16 <sup>2</sup>Centre for Synthetic and Systems Biology, University of Edinburgh, EH9 3BF, UK.

17 <sup>3</sup>Institute of Quantitative Biology, Biochemistry and Biotechnology, School of Biological  
18 Sciences, University of Edinburgh, EH9 3FF, UK.

19 <sup>4</sup>School of Biological Sciences, University of East Anglia, Norwich, NR4 7TJ, UK.

20 <sup>5</sup>Australian Institute of Bioengineering and Nanotechnology, The University of Queensland,  
21 Brisbane, Queensland 4072, Australia

22 <sup>6</sup>CSIRO, Synthetic Biology Future Science Platform, Brisbane, Queensland, 4001, Australia.

23 <sup>7</sup>Department of Biochemistry, University of Cambridge, CB2 1QW, UK.

24

25 *One sentence summary:* Development of a Golden Gate-based assembly standard for cloning  
26 and transformation in cyanobacteria that is compatible with, and builds on, the broadly  
27 established plant modular cloning syntax.

28

29 *Author Contributions:* RV, GARG, AAS and AM designed the study with input from BW; RV,  
30 GARG, AAS, AP, JM, MDG, KV performed experiments; VZ designed online software; BW  
31 contributed research reagents and materials. AM prepared the manuscript with input from  
32 experimentalists and BW, CJH and DL-S.

33 **ABSTRACT (250 word limit)**

34 Recent advances in synthetic biology research have been underpinned by an exponential  
35 increase in available genomic information and a proliferation of advanced DNA assembly  
36 tools. The adoption of plasmid vector assembly standards and parts libraries has greatly  
37 enhanced the reproducibility of research and exchange of parts between different labs and  
38 biological systems. However, a standardised Modular Cloning (MoClo) system is not yet  
39 available for cyanobacteria, which lag behind other prokaryotes in synthetic biology despite  
40 their huge potential in biotechnological applications. By building on the assembly library and  
41 syntax of the Plant Golden Gate MoClo kit, we have developed a versatile system called  
42 CyanoGate that unites cyanobacteria with plant and algal systems. Here we have generated a  
43 suite of parts and acceptor vectors for making i) marked/unmarked knock-outs or integrations  
44 using an integrative acceptor vector, and ii) transient multigene expression and repression  
45 systems using known and novel replicative vectors. We have tested and compared the  
46 CyanoGate system in the established model cyanobacterium *Synechocystis* sp. PCC 6803 and  
47 the more recently described fast-growing strain *Synechococcus elongatus* UTEX 2973. We  
48 observed that fast-growth phenotype in UTEX 2973 is only evident under specific growth  
49 conditions, but that UTEX 2973 can accumulate high levels of proteins with strong native or  
50 synthetic promoters. The system is publicly available and can be readily expanded to  
51 accommodate other standardised MoClo parts to accelerate the development of reliable  
52 synthetic biology tools for the cyanobacterial community.

53

54 **INTRODUCTION**

55 Much work is focused on expanding synthetic biology approaches to engineer photosynthetic  
56 organisms, including cyanobacteria. Cyanobacteria are an evolutionarily ancient and diverse  
57 phylum of photosynthetic prokaryotic organisms that are ecologically important, and are  
58 thought to contribute *ca.* 25% to oceanic net primary productivity (Castenholz, 2001;  
59 Flombaum et al., 2013). The chloroplasts of all photosynthetic eukaryotes, including plants,  
60 resulted from the endosymbiotic uptake of a cyanobacterium by a eukaryotic ancestor (Keeling,  
61 2004). Therefore, cyanobacteria have proved useful as model organisms for the study of  
62 photosynthesis, electron transport and associated biochemical pathways, many of which are  
63 conserved in eukaryotic algae and higher plants. Several unique aspects of cyanobacterial  
64 photosynthesis, such as the biophysical carbon concentrating mechanism, also show promise  
65 as a means for enhancing productivity in crop plants (Rae et al., 2017). Furthermore,  
66 cyanobacteria are increasingly recognized as valuable platforms for industrial biotechnology

67 to convert CO<sub>2</sub> and H<sub>2</sub>O into valuable products using solar energy (Tan et al., 2011; Ducat et  
68 al., 2011; Ramey et al., 2015). They are metabolically diverse and encode many components  
69 (e.g. P450 cytochromes) necessary for generating high-value pharmaceutical products that can  
70 be challenging to produce in other systems (Nielsen et al., 2016; Wlodarczyk et al., 2016; Pye  
71 et al., 2017; Stensjö et al., 2017). Furthermore, cyanobacteria show significant promise in  
72 biophotovoltaic devices for generating electrical energy (McCormick et al., 2015; Saar et al.,  
73 2018).

74

75 Based on morphological complexity, cyanobacteria are classified into five sub-sections (I-V)  
76 (Castenholz, 2001). Several members of the five sub-sections have been reportedly transformed  
77 (Vioque, 2007; Stucken et al., 2012), suggesting that many cyanobacterial species are amenable  
78 to genetic manipulation. Exogenous DNA can be integrated into or removed from the genome  
79 through homologous recombination-based approaches using natural transformation,  
80 conjugation (tri-parental mating), or electroporation (Heidorn et al., 2011). Exogenous DNA  
81 can also be propagated by replicative vectors, although the latter are currently restricted to the  
82 use of a single vector-type based on the broad-host range RSF1010 origin (Mermet-Bouvier et  
83 al., 1993; Huang et al., 2010; Taton et al., 2014). Transformation tools have been developed  
84 for generating “unmarked” mutant strains (lacking an antibiotic resistance marker cassette) in  
85 several model species, such as *Synechocystis* sp. PCC 6803 (*Synechocystis* hereafter) (Lea-  
86 Smith et al., 2016). More recently, markerless genome editing using CRISPR-based  
87 approaches has been demonstrated to function in both unicellular and filamentous strains  
88 (Ungerer and Pakrasi, 2016; Wendt et al., 2016).

89

90 Although exciting progress is being made in developing effective transformation systems,  
91 cyanobacteria still lag behind in the field of synthetic biology compared to bacterial  
92 (heterotrophic), yeast and mammalian systems. Relatively few broad-host range genetic parts  
93 have been characterised, but many libraries of parts for constructing regulatory modules and  
94 circuits are starting to become available, albeit using different standards, which makes them  
95 difficult to combine (Huang and Lindblad, 2013; Camsund et al., 2014; Albers et al., 2015;  
96 Markley et al., 2015; Englund et al., 2016; Kim et al., 2017; Immethun et al., 2017; Taton et  
97 al., 2017; Ferreira et al., 2018; Li et al., 2018; Liu and Pakrasi, 2018; Wang et al., 2018). One  
98 key challenge is clear: parts that are widely used in *Escherichia coli* behave very differently in  
99 model cyanobacterial species, such as *Synechocystis* (Heidorn et al., 2011). Furthermore,  
100 different cyanobacterial strains generally show a wide variation for functionality and

101 performance of different genetic parts (e.g. promoters, reporter genes and antibiotic resistance  
102 markers) (Taton et al., 2014; Englund et al., 2016; Kim et al., 2017; Taton et al., 2017). This  
103 suggests that parts need to be validated, calibrated, and perhaps modified, for individual strains,  
104 including model species and strains that may be more commercially relevant. Rapid cloning  
105 and assembly methods are essential for accelerating the ‘design, build, test and learn’ cycle,  
106 which is a central tenet of synthetic biology (Nielsen and Keasling, 2016).

107

108 The adoption of new cloning and vector assembly methods (e.g. Isothermal (Gibson) Assembly  
109 and MoClo), assembly standards and part libraries has greatly enhanced the scalability of  
110 synthetic biology-based approaches in a range of biological systems (Moore et al., 2016;  
111 Vazquez-Vilar et al., 2018). Recent advances in synthetic biology have led to the development  
112 of standards for Type IIS restriction endonuclease-mediated assembly (commonly known as  
113 Golden Gate cloning) for several model systems, including plants (Sarrion-Perdigones et al.,  
114 2013; Engler et al., 2014; Andreou and Nakayama, 2018). Based on a common Golden Gate  
115 Modular Cloning (MoClo) syntax, large libraries are now available for fusion of different  
116 genetic parts to assemble complex vectors cheaply and easily without proprietary tools and  
117 reagents (Patron et al., 2015). High-throughput and automated assembly are projected to be  
118 widely available soon through DNA synthesis and construction facilities, such as the UK DNA  
119 Synthesis Foundries, where MoClo is seen as the most suitable assembly standard (Chambers  
120 et al., 2016).

121

122 Here we have developed an easy-to-use system called CyanoGate that unites cyanobacteria  
123 with plant and algal systems, by building on the established Golden Gate MoClo syntax and  
124 assembly library for plants (Engler et al., 2014) that has been adopted by the OpenPlant  
125 consortium ([www.openplant.org](http://www.openplant.org)), iGEM competitions as “Phytobricks” and the MoClo kit for  
126 the microalga *Chlamydomonas reinhardtii* (Crozet et al., 2018). Firstly, we have constructed  
127 and characterised a suite of known and novel genetic parts (level 0) for use in cyanobacterial  
128 research, including promoters, terminators, antibiotic resistant markers, neutral sites and gene  
129 repression systems (Na et al., 2013; Yao et al., 2015; Sun et al., 2018). Secondly, we have  
130 designed an additional level of acceptor vectors (level T) to facilitate integrative or replicative  
131 transformation. We have characterised assembled level T vectors in *Synechocystis* and in  
132 *Synechococcus elongatus* UTEX 2973 (UTEX 2973 hereafter), which has a reported doubling  
133 time similar to that of *Saccharomyces cerevisiae* under specific growth conditions (Yu et al.,

134 2015; Ungerer et al., 2018a; 2018b). Lastly, we have developed an online tool for assembly of  
135 CyanoGate and Plant MoClo vectors to assist with the adoption of the CyanoGate system.

136

## 137 **MATERIALS AND METHODS**

### 138 **Cyanobacterial culture conditions**

139 Cyanobacterial strains of *Synechocystis*, UTEX 2973 and *Synechococcus elongatus* PCC 7942  
140 (PCC 7942 hereafter) were maintained on 1.5% (w/v) agar plates containing BG11 medium.  
141 Liquid cultures were grown in Erlenmeyer flasks (100 ml) containing BG11 medium (Rippka  
142 et al., 1979) supplemented with 10 mM NaHCO<sub>3</sub>, shaken at 100 rpm and aerated with filter-  
143 sterilised water-saturated atmospheric air. *Synechocystis* and PCC 7942 strains were grown at  
144 30°C with continuous light (100 μmol photons m<sup>-2</sup> s<sup>-1</sup>) and UTEX 2793 strains were grown at  
145 40°C with 300 μmol photons m<sup>-2</sup> s<sup>-1</sup> in an Infors Multitron-Pro supplied with warm white LED  
146 lighting (Infors HT).

147

### 148 **Growth analysis**

149 Growth of *Synechocystis*, UTEX 2973 and PCC 7942 was measured in a Photon Systems  
150 Instrument Multicultivator MC 1000-OD (MC). Starter cultures were grown in a Photon  
151 Systems Instrument AlgaeTron AG 230 at 30°C under continuous warm-white light (100 μmol  
152 photons m<sup>-2</sup> s<sup>-1</sup>) with air bubbling and shaken at 160 rpm unless otherwise indicated. These  
153 were grown to an optical density at 750 nm (OD<sub>750</sub>) of approximately 1.0, and used to seed 80  
154 ml cultures for growth in the MC at a starting OD<sub>720</sub> of ~0.2 (the MC measures culture growth  
155 at OD<sub>720</sub>). Cultures were then grown under continuous warm-white light at 30°C (300 μmol  
156 photons m<sup>-2</sup> s<sup>-1</sup>) with air bubbling or 30°C (under 300 or 500 μmol photons m<sup>-2</sup> s<sup>-1</sup>) or 41, 45  
157 and 50°C (500 μmol photons m<sup>-2</sup> s<sup>-1</sup>) with 5% CO<sub>2</sub> bubbling until the fastest grown strain was  
158 at OD<sub>720</sub> = ~0.9, the maximum accurate OD that can be measured with this device. A total of  
159 5-6 replicate experiments were performed over two separate runs (16 in total), each inoculated  
160 from a different starter culture.

161

### 162 **Vector construction**

#### 163 *Level 0 vectors*

164 Native cyanobacterial genetic parts were amplified from genomic DNA using NEB Q5 High-  
165 Fidelity DNA Polymerase (New England Biolabs) (**Fig. 1; Supplementary Table S1**). Where  
166 necessary, native genetic parts were domesticated (i.e. *BsaI* and *BpiI* sites were removed) using

167 specific primers. Alternatively, parts were synthesised as Gblocks<sup>®</sup> DNA fragments (Integrated  
168 DNA Technology) and cloned directly into an appropriate level 0 acceptor (see  
169 **Supplementary Information S1** for vector maps) (Engler et al. 2014).

170

171 Golden Gate assembly reactions were performed with restriction enzymes *Bsa*I (New England  
172 Biolabs) or *Bpi*I (Thermofisher), and T4 DNA ligase (Thermofisher) (see **Supplementary**  
173 **Information S2-S4** for detailed protocols). Vectors were transformed into One Shot TOP10  
174 chemically competent *Escherichia coli* (Thermofisher) as per the manufacturer's instructions.  
175 Transformed cultures were grown at 37°C on [1.5% (w/v)] LB agar plates or in liquid LB  
176 medium shaking at 260 rpm, with appropriate antibiotic selection for level 0, 1, M and P vectors  
177 as outlined in Engler et al. (2014).

178

#### 179 *Level T acceptor vectors and new level 0 acceptors*

180 A new level T vector system was designed that provides MoClo-compatible replicative vectors  
181 or integrative vectors for genomic modifications in cyanobacteria (Heidorn et al., 2011) (**Fig.**  
182 **2; Supplementary Table S1; Supplementary Information S1**). For replicative vectors, we  
183 modified the pPMQAK1 carrying an RSF1010 replicative origin (Huang et al., 2010) to make  
184 pPMQAK1-T, and vector pSEVA421 from the Standard European Vector Architecture  
185 (SEVA) 2.0 database ([seva.cnb.csic.es](http://seva.cnb.csic.es)) carrying the RK2 replicative origin to make  
186 pSEVA421-T (Silva-Rocha et al., 2013). Replicative vector backbones were domesticated to  
187 remove native *Bsa*I and *Bpi*I sites where appropriate. The region between the BioBrick's prefix  
188 and suffix was then replaced by a *lacZ* expression cassette flanked by two *Bpi*I sites that  
189 produce overhangs TGCC and GGGA, which are compatible with the plant Golden Gate  
190 MoClo assembly syntax for level 2 acceptors (e.g. pAGM4673) (Engler et al., 2014). For  
191 integrative vectors, we domesticated a pUC19 vector backbone and introduced two *Bpi*I sites  
192 compatible with a level 2 acceptor (as above) to make pUC19A-T and pUC19S-T. In addition,  
193 we made a new low copy level 0 acceptor (pSC101 origin of replication) for promoter parts  
194 based on the BioBrick standard vector pSB4K5 (Liu et al., 2018). DNA was amplified using  
195 NEB Q5 High-Fidelity DNA Polymerase (New England Biolabs). All vectors were sequenced  
196 following assembly to confirm domestication and the integrity of the MoClo cloning site.

197

#### 198 *Level 0 parts for CRISPRi and srRNA*

199 A nuclease deficient Cas9 gene sequence sourced from Addgene ([www.addgene.org/44249/](http://www.addgene.org/44249/))  
200 was domesticated and assembled as a level 0 CDS part (**Supplementary Table S1; S2**) (Qi et

201 al., 2013). Five promoters of different strengths were truncated to the transcriptional start site  
202 (TSS) and cloned into a new level 0 acceptor vector with the unique overhangs GGAG and  
203 TAGC (**Fig. 1**). Two new level 0 parts with the unique overhangs GTTT and CGCT were  
204 generated for the sgRNA scaffold and srRNA HFQ handle (based on MicC) (Na et al., 2013),  
205 respectively. Assembly of level 1 expression cassettes proceeded by combining appropriate  
206 level 0 parts with a PCR product for either a srRNA or sgRNA (**Fig. 1**).

207

### 208 **Cyanobacterial transformation and conjugation**

209 Transformation with integrative level T vectors was performed as in Lea-Smith et al. (2016).  
210 For transformation by electroporation, cultures were harvested during the ‘exponential’ growth  
211 phase (OD<sub>750</sub> of ~0.6) by centrifugation at 4,000 g for 10 min. The cell pellet was washed 3  
212 times with 2 ml of sterile 1 mM HEPES buffer (pH 7.5), re-suspended in water with 3-5 µg of  
213 level T vector DNA and transferred into a 0.1 cm electroporation cuvette (Scientific Laboratory  
214 Suppliers). Re-suspended cells were electroporated using an Eppendorf 2510 electroporator  
215 (Eppendorf) set to 1200 V. Sterile BG-11 (1 ml) was immediately added to the electroporated  
216 cells. Following a 1 hr incubation at RT, the cells were plated on 1.5% (w/v) agar plates  
217 containing BG-11 with antibiotics at standard working concentrations to select for transformed  
218 colonies. The plates were sealed with parafilm and placed under 15 µmol photons m<sup>-2</sup> s<sup>-1</sup> light  
219 at 30°C for 1 day. The plates were then moved to 30 µmol photons m<sup>-2</sup> s<sup>-1</sup> light until colonies  
220 appeared. After 15-20 days, putative transformants were recovered and streaked onto new  
221 plates with appropriate antibiotics for further study.

222

223 Genetic modification by conjugation in *Synechocystis* was facilitated by an *E. coli* strain  
224 (HB101) carrying both mobilizer and helper vectors pRK2013 (ATCC® 37159™) and pRL528  
225 ([www.addgene.org/58495/](http://www.addgene.org/58495/)), respectively (Tsinoremas et al., 1994). For UTEX 2973,  
226 conjugation was facilitated by a MC1061 strain carrying mobilizer and helper vectors pRK24  
227 ([www.addgene.org/51950/](http://www.addgene.org/51950/)) and pRL528, respectively. Cultures of HB101 and OneShot  
228 TOP10 *E. coli* strains carrying level T cargo vectors were grown for approximately 15 hr with  
229 appropriate antibiotics. Cyanobacterial strains were grown to an OD<sub>750</sub> of ~1. All bacterial  
230 cultures were washed three times with either fresh LB medium for *E. coli* or BG11 for  
231 cyanobacteria prior to use. *Synechocystis* cultures (100 µl, OD<sub>750</sub> of 0.5-0.8) were conjugated  
232 by combining appropriate HB101 and the cargo strains (100 µl each) and plating onto HATF  
233 0.45 µm transfer membranes (Merck Millipore) placed on LB: BG11 (1: 19) agar plates. For  
234 UTEX 2973 conjugations, appropriate MC1061 and the cargo strains (100 µl each) were



235 initially combined and incubated at 30°C for 30 min, then mixed with UTEX 2973 cultures  
236 (100 µl, OD<sub>750</sub> of 0.5-0.8) and incubated at 30°C for 2 hr, and then plated onto transfer  
237 membranes as above. *Synechocystis* and UTEX 2973 transconjugates were grown under  
238 culturing conditions outlined above. Following growth on non-selective media for 24 hr, the  
239 membranes were transferred to BG11 agar plates supplemented with appropriate antibiotics.  
240 Colonies were observed within a week for both strains. Chlorophyll content of wild-type (WT)  
241 and mutant strains was calculated as in Lea-Smith et al. (2013).

242

### 243 **Fluorescence assays**

244 Transgenic strains maintained on agar plates containing appropriate antibiotics were used to  
245 inoculate 10 ml seed cultures that were grown to an optical density at 750 nm (OD<sub>750</sub>) of  
246 approximately 1.0, as measured with a WPA Biowave II spectrometer (Biochrom). Seed  
247 cultures were diluted to an OD<sub>750</sub> of 0.2, and 2 ml starting cultures were transferred to 24-well  
248 plates (Costar® Corning Incorporated) for experiments. *Synechocystis* and UTEX 2973 strains  
249 were grown in an Infors Multitron-Pro in the same culturing conditions described above. OD<sub>750</sub>  
250 was measured using a FLUOstar OMEGA microplate reader (BMG Labtech). Fluorescence of  
251 eYFP for individual cells (10,000 cells per culture) was measured by flow cytometry using an  
252 Attune NxT Flow Cytometer (ThermoFisher). Cells were gated using forward and side scatter,  
253 and median eYFP fluorescence was calculated from excitation/emission wavelengths 488  
254 nm/515–545 nm (Kelly et al., 2018) and reported at 48 hr unless otherwise stated.

255

### 256 **Cell counts, soluble protein and eYFP quantification**

257 *Synechocystis* and UTEX 2973 strains were cultured for 48 hr as described above, counted  
258 using a haemocytometer and then harvested for soluble protein extraction. Cells were pelleted  
259 by centrifugation at 4,000 g for 15 min, re-suspended in lysis buffer [0.1 M potassium  
260 phosphate buffer (pH 7.0), 2 mM DTT and one Roche cComplete EDTA-free protease inhibitor  
261 tablet per 10 ml (Roche Diagnostics)] and lysed with 0.5 mm glass beads (Thistle Scientific)  
262 in a TissueLyser II (Qiagen). The cell lysate was centrifuged at 18,000 g for 30 min and the  
263 supernatant assayed for soluble protein content using Pierce 660nm Protein Assay Reagent  
264 against BSA standards (Thermo Fisher Scientific). Extracts were subjected to sodium dodecyl  
265 sulfate–polyacrylamide gel electrophoresis (SDS-PAGE) in a 4–12% (w/v) polyacrylamide gel  
266 (Bolt® Bis-Tris Plus Gel; Thermo Fisher Scientific) alongside a SeeBlue Plus2 Prestained  
267 protein ladder (Thermo), transferred to polyvinylidene fluoride (PVDF) membrane then probed  
268 with monoclonal anti-GFP serum (AbCAM) at 1: 1,000 dilution, followed by LI-COR IRDye

269 @800CW goat anti-rabbit IgG (LI-COR Inc.) at 1: 10,000 dilution, then viewed on an LI-COR  
270 Odyssey CLx Imager. eYFP protein content was estimated by immunoblotting using  
271 densitometry using LI-COR Lite Studio software v5.2 . Relative eYFP protein abundance was  
272 estimated by densitometry using LI-COR Lite Studio software v5.2.

273

### 274 **Plasmid vector and genome copy number determination**

275 The genome copy number and copy number of heterologous self-replicating plasmid vectors  
276 in *Synechocystis* was estimated using a real-time quantitative PCR (RT-qPCR) approach  
277 adapted from Zerulla et al. (2016). Cytoplasmic extracts containing total cellular DNA were  
278 harvested from *Synechocystis* cultures after 48 hr growth ( $OD_{750} = ca. 5$ ) according to Zerulla  
279 et al. (2016). Cells in 10 ml of culture were pelleted by centrifugation at 4,000 g for 15 min,  
280 disrupted by shaking at 30 Hz for 10 min in a TissueLyser II with a mixture of 0.2 mm and 0.5  
281 mm acid washed glass beads (0.35 g each), and then resuspended in dH<sub>2</sub>O. The culture cell  
282 count was determined prior to harvest using a haemocytometer and checked again after cell  
283 disruption to calculate the efficiency of cell disruption. A standard curve based on a dilution  
284 series of vector DNA was generated and used for RT-qPCR analysis in parallel with extracts  
285 carrying the same vector. Two DNA fragments (*ca.* 1 kb) targeting two separate loci (*petB* and  
286 *secA*) were amplified from isolated genomic DNA from *Synechocystis* using standard PCR  
287 (Pinto et al., 2012). DNA mass concentrations were determined photometrically and the  
288 concentrations of DNA molecules was calculated from the known molecular mass. As above,  
289 a standard curve based on a dilution series of the two fragments was generated to estimate  
290 genome copy number in the extracts (Zerulla et al., 2016). The Ct of the extracts were then  
291 plotted against the linear portion of the standard curves to estimate plasmid vector copy number  
292 and genome copy number per cell. Oligonucleotides used are summarised in **Supplementary**  
293 **Table S3.**

294

### 295 **Confocal laser scanning microscopy**

296 Cultures were imaged using Leica TCS SP8 confocal microscopy (Leica Microsystems) with  
297 a water immersion objective lens (HCX APO L 20x/0.50 W). Excitation/emission wavelengths  
298 were 514 nm/527–546 nm for eYFP and 514 nm/605–710 nm for chlorophyll autofluorescence.

299

## 300 **RESULTS AND DISCUSSION**

### 301 **Construction of the CyanoGate system**

302 The CyanoGate system integrates with the two-part Golden Gate MoClo Plant Tool Kit, which  
303 can be acquired from Addgene [standardised parts (Kit #1000000047) and backbone acceptor  
304 vectors (Kit # 1000000044), ([www.addgene.org](http://www.addgene.org))] (Engler et al., 2014). A comparison of the  
305 benefits of MoClo- and Gibson assembly-based cloning strategies is shown in **Supplementary**  
306 **Information S5**. The syntax for level 0 parts was adapted for prokaryotic cyanobacteria to  
307 address typical cloning requirements for cyanobacterial research (**Fig. 1**). New level 0 parts  
308 were assembled from a variety of sources (**Supplementary Table S1**). Level 1, M and P  
309 acceptor vectors were adopted from the MoClo Plant Tool Kit, which facilitates assembly of  
310 level 0 parts in a level 1 vector, and subsequently up to seven level 1 modules in level M. Level  
311 M assemblies can be combined further into level P and cycled back into level M to produce  
312 larger multi-module vectors if required (**Supplementary Information S3**). Vectors >50 kb in  
313 size assembled by MoClo have been reported (Werner et al., 2012). Modules from level 1 or  
314 level P can be assembled in new level T vectors designed for cyanobacterial transformation  
315 (**Fig. 2**). We found that both UTEX 2973 and *Synechocystis* produced recombinants following  
316 electroporation or conjugation methods with level T vectors. For the majority of the work  
317 outlined below, we relied on the conjugation approach.

318

### 319 **Integration - generating marked and unmarked knockout mutants**

320 A common method for engineering stable genomic knock out and knock in mutants in several  
321 cyanobacteria relies on homologous recombination via integrative (suicide) vectors using a  
322 two-step marked-unmarked strategy (Lea-Smith et al., 2016) (**Supplementary Information**  
323 **S4**). Saar et al., 2018 recently used this approach to introduce up to five genomic alterations  
324 into a single *Synechocystis* strain. Firstly, marked mutants are generated with an integrative  
325 vector carrying two sequences (approximately 1 kb each) identical to the regions of the  
326 cyanobacterial chromosome flanking the deletion/insertion site. Two gene cassettes are  
327 inserted between these flanking sequences: a levansucrase expression cassette (*sacB*) that  
328 confers sensitivity to transgenic colonies grown on sucrose and an antibiotic resistance cassette  
329 ( $Ab^R$ ) of choice. Secondly, unmarked mutants (carrying no selection markers) are generated  
330 from fully segregated marked lines using a separate integrative vector carrying only the  
331 flanking sequences and selection on plates containing sucrose.

332

333 We adapted this approach for the CyanoGate system (**Fig. 1**). To generate level 1 vectors for  
334 making knock out mutants, sequences flanking the upstream (UP FLANK) and downstream  
335 (DOWN FLANK) site of recombination were ligated into the plant MoClo Prom+5U (with

336 overhangs GGAG-AATG), and 3U+Ter (GCTT-CGCT) positions, respectively, to generate  
337 new level 0 parts (**Fig. 1B**). In addition, full expression cassettes were made for sucrose  
338 selection (*sacB*) and antibiotic resistance ( $Ab^R$ Spec,  $Ab^R$ Kan and  $Ab^R$ Ery) in level 0 that ligate  
339 into positions SP (AATG-AGGT) and CDS2 (stop) (AGGT-GCTT), respectively. Marked  
340 level 1 modules can be assembled using UP FLANK, DOWN FLANK, *sacB* and the required  
341  $Ab^R$  level 0 part. For generating the corresponding unmarked level 1 module, a short 59 bp  
342 linker (UNMARK LINKER) can be ligated into the CDS1ns (AATG-GCTT) position for  
343 assembly with an UP FLANK and DOWN FLANK (**Fig. 1D**). Unmarked and marked level 1  
344 modules can then be assembled into level T integrative vectors, with the potential capacity to  
345 include multiple knockout modules in a single level T vector.

346  
347 To validate our approach, we constructed the level 0 flanking vectors pC0.024 and pC0.025  
348 and assembled two level T integrative vectors using pUC19-T (*cpcBA*-M and *cpcBA*-UM, with  
349 and without the *sacB* and  $Ab^R$  cassettes, respectively) to remove the *cpcBA* promoter and  
350 operon in *Synechocystis* and generate an “Olive” mutant unable to produce the phycobiliprotein  
351 C-phycocyanin (Kirst et al., 2014; Lea-Smith et al., 2014) (**Fig. 3; Supplementary Table S1**).  
352 Following transformation with *cpcBA*-M, we successfully generated a marked  $\Delta cpcBA$  mutant  
353 carrying the *sacB* and the  $Ab^R$ Kan cassettes after selective segregation (*ca.* 3 months) (**Fig.**  
354 **3A**). The unmarked  $\Delta cpcBA$  mutant was then isolated following transformation of the marked  
355  $\Delta cpcBA$  mutant with *cpcBA*-UM and selection on sucrose (*ca.* 2 weeks) (**Fig. 3B**). Absence of  
356 C-phycocyanin in the Olive mutant resulted in a characteristic drop in absorbance at 625 nm  
357 (**Fig. 3D**) and a significant reduction in chlorophyll content compared to WT cells ( $28.4 \pm 0.2$   
358 and  $48.3 \pm 0.2$  amol chl cell<sup>-1</sup>, respectively) (Kirst et al., 2014; Lea- Smith et al., 2014).

359

### 360 **Generating knock in mutants**

361 Flexibility in designing level 1 insertion cassettes is needed when making knock in mutants.  
362 Thus, for knock in mutants the upstream and downstream sequences flanking the insertion site,  
363 and any required expression or marker cassettes, are first assembled into separate level 1  
364 modules from UP FLANK and DOWN FLANK level 0 parts (**Fig. 1E, F**). Seven level 1  
365 modules can be assembled directly into Level T (**Fig. 2**), thus with a single pair of flanking  
366 sequences up to five level 1 expression cassettes could be included in a Level T vector.

367

368 Linker parts (20 bp) UP FLANK LINKER and DOWN FLANK LINKER were generated to  
369 allow assembly of level 0 UP FLANK and DOWN FLANK parts into separate level 1 acceptor

370 vectors. Similarly, level 0 linker parts were generated for *sacB* and Ab<sup>R</sup> (**Fig. 1H, I**). Level 1  
371 vectors at different positions can then be assembled in level T (or M) containing one or more  
372 expression cassettes, an Ab<sup>R</sup> of choice, or both *sacB* and Ab<sup>R</sup> (**Fig. 2**).

373

374 Using this approach, CyanoGate can facilitate the generation of knock in mutants using a  
375 variety of strategies. For example, if retention of a resistance marker is not an experimental  
376 requirement (e.g. Liberton et al., 2017), only a single antibiotic resistance cassette needs to be  
377 included in level T. Alternatively, a two-step marked-unmarked strategy could be followed, as  
378 for generating knockout mutants.

379

380 While knock out strategies can target particular loci, knock in approaches often rely on  
381 recombination at designated ‘neutral sites’ within the genome of interest that can be disrupted  
382 with no or minimal impact on growth phenotype (Ng et al., 2015; Pinto et al., 2015). Based on  
383 loci reported in the literature, we have assembled a suite of flanking regions to target neutral  
384 sites in *Synechocystis* (designated 6803 NS1-4) (Pinto et al., 2015), *Synechococcus* sp. PCC  
385 7002 (PCC 7002 hereafter) (designated 7002 NS1 and NS2) (Ruffing et al., 2016; Vogel et al.,  
386 2017), and neutral sites common to UTEX 2973, PCC 7942 and *Synechococcus elongatus* PCC  
387 6301 (designated 7942 NS1-3) (Bustos and Golden, 1992; Kulkarni and Golden, 1997;  
388 Andersson et al., 2000; Niederholtmeyer et al., 2010) (**Supplementary Table S1**). Pinto et al.  
389 (2015) have qualitatively compared the impact of the four *Synechocystis* neutral sites  
390 assembled here under several different growth conditions, and observed that insertions at 6803  
391 NS3 and NS4 had no significant effect on growth compared to WT cultures, while insertions  
392 at NS2 and NS1 had small but significant effects depending on the growth conditions. Several  
393 studies have used 6803 NS3, for example, to engineer a *Synechocystis* strain for the  
394 bioremediation of microcystins (Dexter et al., 2018) and the development of T7 polymerase-  
395 based synthetic promoter systems (Ferreira et al., 2018). For the two PCC 7002 neutral sites,  
396 growth rates with insertions at 7002 NS1 were slightly reduced (Vogel et al., 2017), but not  
397 significantly affected with insertions at 7002 NS2 (Ruffing et al., 2016). Insertions at the three  
398 7942 neutral sites reportedly have no phenotypic effect on morphology or growth rate (Clerico  
399 et al., 2007; Niederholtmeyer et al., 2010) and have been used to study mRNA stability and  
400 translation (Kulkarni and Golden, 1997), circadian rhythms (Anderson et al. 2000),  
401 chromosome duplication (Watanabe et al., 2017) and to engineer PCC 7942 for synthesising  
402 heterologous products (Niederholtmeyer et al., 2010; Gao et al., 2016). When using the neutral  
403 sites supplied with CyanoGate (or others), we would still recommend a thorough growth

404 analysis under the specific culturing conditions being tested to identify any potential impact of  
405 the inserted DNA on growth phenotype.

406

407 To validate our system, we generated a level T vector carrying the flanking regions for the  
408 *cpcBA* operon and an eYFP expression cassette (*cpcBA*-eYFP) (**Fig. 4A, B; Supplementary**  
409 **Table S1**). We successfully transformed this vector into our marked “Olive” *Synechocystis*  
410 mutant, to generate a stable olive mutant with constitutive expression of eYFP (Olive-eYFP)  
411 (**Fig. 4C**).

412

### 413 **Expression comparison for promoter parts in *Synechocystis* and UTEX 2973**

414 We constructed level 0 parts for a wide selection of synthetic promoters and promoters native  
415 to *Synechocystis*. Promoters were assembled as expression cassettes driving eYFP in  
416 replicative level T vector pPMQAK1-T to test for differences in expression when conjugated  
417 into *Synechocystis* or UTEX 2973. We first compared the growth rates of *Synechocystis*, UTEX  
418 and PCC 7942 [a close relative of UTEX 2973 (Yu et al., 2015)] under a variety of different  
419 culturing conditions (**Supplementary Figure S1**). We found that growth rates were  
420 comparable between *Synechocystis* and PCC 7942 at temperatures below 40°C regardless of  
421 light levels and supplementation with CO<sub>2</sub>. In contrast, UTEX 2973 grew poorly under those  
422 conditions. UTEX 2973 only showed an enhanced growth rate at 45°C under the highest light  
423 tested (500 μmol photons m<sup>-2</sup> s<sup>-1</sup>) with CO<sub>2</sub>, while all three strains failed to grow at 50°C. These  
424 results confirm that the enhanced growth phenotype reported for UTEX 2973 requires specific  
425 conditions as reported by Ungerer et al. (2018a; 2018b). Furthermore, they are consistent with  
426 recent reports that this phenotype is linked to an increased stress tolerance, which has been  
427 attributed to a small number of nucleotide polymorphisms (Lou et al., 2018; Ungerer et al.,  
428 2018b). We proceeded with CyanoGate part characterisations and comparisons under the best  
429 conditions achievable for *Synechocystis* and UTEX 2973 (see Materials and Methods)  
430 (**Supplementary Figure S2A**).

431

#### 432 *Promoters native to Synechocystis*

433 We assembled several previously reported promoters from *Synechocystis* in the CyanoGate kit.  
434 These include six inducible/repressible promoters (*P<sub>nrsB</sub>*, *P<sub>coaT</sub>*, *P<sub>nirA</sub>*, *P<sub>petE</sub>*, *P<sub>isiAB</sub>*, and *P<sub>arsB</sub>*),  
435 which were placed in front of the strong, synthetic *Synechocystis* ribosomal binding site (RBS\*)  
436 (Heidorn et al., 2011) as used in Englund et al. (2016) (**Supplementary Table S1;**  
437 **Supplementary Information S1**). *P<sub>nrsB</sub>* and *P<sub>coaT</sub>* drive the expression of nickel and cobalt ion

438 efflux pumps and are induced by  $\text{Ni}^{2+}$ , and  $\text{Co}^{2+}$  or  $\text{Zn}^{2+}$ , respectively (Peca et al., 2008; Blasi  
439 et al., 2012; Guerrero et al., 2012; Englund et al., 2016).  $P_{\text{nirA}}$ , from the nitrate assimilation  
440 operon, is induced by the presence of  $\text{NO}_3^-$  and/or  $\text{NO}_2^-$  (Kikuchi et al., 1996; Qi et al., 2005).  
441  $P_{\text{petE}}$  drives the expression of plastocyanin and is induced by  $\text{Cu}^{2+}$ , which has previously been  
442 used for the expression of heterologous genes (Guerrero et al., 2012; Camsund et al., 2014).  
443 The promoter of the *isiAB* operon ( $P_{\text{isiAB}}$ ) is repressed by  $\text{Fe}^{3+}$  and activated when the cell is  
444 under iron stress (Kunert et al., 2003).  $P_{\text{arsB}}$  drives the expression of a putative arsenite and  
445 antimonite carrier and is activated by  $\text{AsO}_2^-$  (Blasi et al., 2012).

446

447 We also cloned the *rnpB* promoter,  $P_{\text{rnpB}}$ , from the Ribonuclease P gene (Huang et al., 2010),  
448 a long version of the *psbA2* promoter,  $P_{\text{psbA2L}}$ , from the Photosystem II protein D1 gene  
449 (Lindberg et al., 2010; Englund et al., 2016) and the promoter of the C-phycoyanin operon,  
450  $P_{\text{cpc560}}$  (also known as  $P_{\text{cpcB}}$  and  $P_{\text{cpcBA}}$ ) (Zhou et al., 2014).  $P_{\text{rnpB}}$  and  $P_{\text{psbA2L}}$  were placed in front  
451 of RBS\* (Heidorn et al., 2011) (**Fig. 5A**). To build on a previous functional characterisation of  
452  $P_{\text{cpc560}}$  (Zhou et al., 2010), we assembled four variants of this strong promoter. Firstly,  $P_{\text{cpc560+A}}$   
453 consisted of the promoter and the 4 bp MoClo overhang AATG. Secondly,  $P_{\text{cpc560}}$  was truncated  
454 by one bp (A), so that that the start codon was aligned with the native  $P_{\text{cpc560}}$  RBS spacer region  
455 length. Zhou et al. (2014) identified 14 predicted transcription factor binding sites (TFBSs) in  
456 the upstream region of  $P_{\text{cpc560}}$  (-556 to -381 bp) and removal of this region resulted in a  
457 significant loss of promoter activity. However, alignment of the reported TFBSs showed their  
458 locations are in the downstream region of the promoter (-180 to -5 bp). We identified 11  
459 additional predicted TFBSs using Virtual Footprint (Munch et al., 2005) in the upstream region  
460 and hypothesised that the promoter activity may be modified by duplicating either of these  
461 regions. So thirdly, we generated  $P_{\text{cpc560\_Dx2}}$  containing a duplicated downstream TFBS region.  
462 For  $P_{\text{cpc560\_Dx2}}$ , only the region between -31 to -180 bp was duplicated to avoid repeating the  
463 Shine-Dalgarno (SD) sequence. Fourthly, we duplicated the upstream region to generate  
464  $P_{\text{cpc560\_Ux2}}$ . We then assembled  $P_{\text{rnpB}}$ ,  $P_{\text{psbA2L}}$  and the four  $P_{\text{cpc560}}$  variants with eYFP and the  
465 *rrnB* terminator ( $T_{\text{rrnB}}$ ) into a Level 1 expression cassette, and subsequently into a level T  
466 replicative vector (pPMQAK1-T) for expression analysis (**Supplementary Table S2**).

467

468 In *Synechocystis* the highest expressing promoter was  $P_{\text{cpc560}}$  (**Fig. 5B**), which indicated that  
469 maintaining the native RBS spacer region for  $P_{\text{cpc560}}$  is important for maximising expression.  
470 Neither  $P_{\text{cpc560\_Dx2}}$  nor  $P_{\text{cpc560\_Ux2}}$  had higher expression levels compared to  $P_{\text{cpc560}}$ .  $P_{\text{cpc560\_Dx2}}$   
471 was strongly decreased compared to  $P_{\text{cpc560}}$ , suggesting that promoter function is sensitive to

472 modification of the downstream region and this region could be a useful target for modulating  
473  $P_{cpc560}$  efficacy. Previous work in *Synechocystis* has suggested that modification of the middle  
474 region of  $P_{cpc560}$  (-380 to -181 bp) may also affect function (Lea-Smith et al., 2014).  $P_{psbA2L}$   
475 produced lower expression levels than any variant of  $P_{cpc560}$  in *Synechocystis*, while  $P_{rnpB}$   
476 produced the lowest expression levels. The observed differences in expression levels are  
477 consistent with those in other studies with *Synechocystis* (Camsund et al., 2014; Englund et al.,  
478 2016; Liu and Pakrasi, 2018).

479

480 In UTEX 2973, the trend in expression patterns was similar to that in *Synechocystis* (**Fig. 5B**).  
481 However, the overall expression levels of eYFP measured in UTEX 2973 were significantly  
482 higher than in *Synechocystis*.  $P_{cpc560}$  was increased by 30%, while  $P_{rnpB}$  showed a 20-fold  
483 increase in expression relative to *Synechocystis*. The relative expression strength of  $P_{psbA2L}$  was  
484 also higher than in *Synechocystis*, and second only to  $P_{cpc560}$  in UTEX 2973. As promoters  
485 derived from  $P_{psbA}$  are responsive to increasing light levels (Englund et al., 2016), the increased  
486 levels of expression for  $P_{psbA2L}$  may be associated with the higher light intensities used for  
487 growing UTEX 2973 compared to *Synechocystis*. Background fluorescence levels were similar  
488 between UTEX 2973 and *Synechocystis* conjugated with an empty pPMQAK1-T vector (i.e.  
489 lacking an eYFP expression cassette), which suggested that the higher fluorescence values in  
490 UTEX 2973 were a direct result of increased levels of eYFP protein.

491

#### 492 *Heterologous and synthetic promoters*

493 A suite of twenty constitutive synthetic promoters was assembled in level 0 based on the  
494 modified BioBricks BBa\_J23119 library of promoters (Markley et al., 2015), and the synthetic  
495  $P_{trc10}$ ,  $P_{tic10}$  and  $P_{tac10}$  promoters (Huang et al., 2010; Albers et al., 2015) (**Supplementary**  
496 **Table S1; Supplementary Information S1**). We retained the broad-range BBa\_B0034 RBS  
497 (AAAGAGGAGAAA) and *lac* operator (*lacO*) from Huang et al. (2010), for future *lacI*-based  
498 repression experiments (*lacI* and the  $P_{lacIQ}$  promoter are included in the CyanoGate kit) (Bhal  
499 et al., 1977). We cloned eight new variants (J23119MH\_V01-8) with mutations in the  
500 canonical BBa\_J23119 promoter sequence (**Fig. 6A**). Additionally, we included the L-  
501 arabinose-inducible promoter from *E. coli* ( $P_{BAD}$ ) (Abe et al., 2014).

502

503 We encountered an unexpected challenge with random internal deletions in the -35 and -10  
504 regions of some promoters of the BBa\_J23119 library and *trc* promoter variants when cloning  
505 them into level 0 acceptors. Similar issues were reported previously for the *E. coli* EcoFlex kit



506 (Moore et al., 2016) that may relate to the functionality of the promoters and the host vector  
507 copy number in *E. coli*, which consequently resulted in cell toxicity and selection for mutated  
508 promoter variants. To resolve this issue, we generated a low copy level 0 promoter acceptor  
509 vector compatible with CyanoGate (pSB4K5 acceptor) for cloning recalcitrant promoters  
510 (**Supplementary Table S1; Supplementary Information S1**). Subsequent assemblies in level  
511 1 and T showed no indication of further mutation.

512

513 We then tested the expression levels of eYFP driven by the synthetic promoters in  
514 *Synechocystis* and UTEX 2973 following assembly in pPMQAK1-T (**Fig. 6B; Supplementary**  
515 **Table S2**). The synthetic promoters showed a 120-fold dynamic range in both cyanobacterial  
516 strains. Furthermore, a similar trend in promoter expression strength was observed ( $R^2 = 0.84$ )  
517 (**Fig. 6C**). However, eYFP expression levels were on average eight-fold higher in UTEX 2973  
518 compared to *Synechocystis*. In *Synechocystis*, the highest expression levels were observed for  
519 J23119 and  $P_{trc10}$ , but these were still approximately 50% lower than values for the native  
520  $P_{cpc560}$  promoters (**Fig. 5B**). The expression trends for the BBa\_J23119 library were consistent  
521 with the subset reported by Camsund et al. (2014) in *Synechocystis*, while the observed  
522 differences between  $P_{trc10}$  and  $P_{cpc560}$  were similar to those reported by Liu and Pakrasi (2018).

523

524 In contrast, the expression levels in UTEX 2973 for J23119 were approximately 50% higher  
525 than  $P_{cpc560}$ . Several synthetic promoters showed expression levels in a similar range to those  
526 for the native  $P_{cpc560}$  promoter variants, including  $P_{trc10}$ , J23111 and the J23119 variant V02.  
527 V02 is identical to J23111 except for an additional 'G' between the -35 and -10 motifs,  
528 suggesting that small changes in the length of this spacer region may not be critical for promoter  
529 strength (similar expression levels were also observed for these two promoters in  
530 *Synechocystis*). In contrast, a single bp difference between J23111 and J23106 in the -35 motif  
531 resulted in an eight- and ten-fold reduction in expression in *Synechocystis* and UTEX 2973,  
532 respectively. The results for UTEX 2973 were unexpected, and to our knowledge no studies to  
533 date have directly compared these promoters in this strain. Recent work has examined the  
534 expression of  $\beta$ -galactosidase using promoters such as  $P_{cpc560}$  and  $P_{trc}$  in UTEX 2973 (Li et al.,  
535 2018). Li et al. (2018) highlighted that different growth environments (e.g. light levels) can  
536 have significant effects on protein expression. Changes in culture density can also affect  
537 promoter activity, such that protein expression levels can change during the exponential and  
538 stationary growth stages depending on the promoter and expression vector used (Ng et al.,  
539 2015; Madsen et al., 2018). Here we tracked eYFP expression levels over time for three days

540 during early and late exponential growth phase for *Synechocystis* and UTEX 2973. Although  
541 expression levels for each promoter fluctuated over time, with peak expression levels at 24 hr  
542 and 48 hr in UTEX 2973 and *Synechocystis*, respectively, the overall expression trends were  
543 generally consistent for the two strains (**Supplementary Figure S2B**).

544

### 545 **Protein expression levels in *Synechocystis* and UTEX 2973**

546 To investigate further the increased levels of eYFP expression observed in UTEX 2973  
547 compared to *Synechocystis*, we examined cell morphology, protein content and eYFP protein  
548 abundances in expression lines for each strain. Confocal image analysis confirmed the coccoid  
549 and rod shapes of *Synechocystis* and UTEX 2973, respectively, and the differences in cell size  
550 (van de Meene et al. 2006; Yu et al., 2015) (**Fig. 7A**). Immunoblot analyses of eYFP from  
551 protein extracts of four eYFP expressing strains correlated well with previous flow cytometry  
552 measurements (**Fig 5; 6**). eYFP driven by the J23119 promoter in UTEX 2973 produced the  
553 highest levels of eYFP protein (**Fig. 7B, C**). Although the density of cells in culture was two-  
554 fold higher in *Synechocystis* compared to UTEX 2973 (**Fig. 7D**), the protein content per cell  
555 was six-fold lower (**Fig. 7E**). We then estimated the average cell volumes for *Synechocystis*  
556 and UTEX 2973 at  $3.91 \pm 0.106 \mu\text{m}^3$  and  $6.83 \pm 0.166 \mu\text{m}^3$  ( $n = 50$  each), respectively, based  
557 on measurements from confocal microscopy images (**Supplementary Figure S3**). Based on  
558 those estimates, we calculated that the density of soluble protein per cell was four-fold higher  
559 in UTEX 2973 compared to *Synechocystis* (**Fig. 7F**). Thus, we hypothesised that the enhanced  
560 levels of eYFP observed in UTEX 2973 were a result of the expression system harnessing a  
561 larger available amino acid pool. Mueller et al. (2017) have reported that UTEX 2973 has an  
562 increased investment in amino acid content compared to PCC 7942, which may be linked to  
563 higher rates of translation in UTEX 2973. Therefore, UTEX 2973 continues to show promise  
564 as a bioplatfrom for generating heterologous protein products, although future work should  
565 study production rates under conditions optimal for faster-growth (Lou et al., 2018; Ungerer et  
566 al., 2018a). Recent characterisation of the UTEX 2973 transcriptome will also assist with native  
567 promoter characterisations (Tan et al., 2017).

568

### 569 **The RK2 origin of replication is functional in *Synechocystis***

570 Synthetic biology tools (e.g. gene expression circuits, CRISPR/Cas-based systems) are often  
571 distributed between multiple plasmid vectors at different copy numbers in order to synthesise  
572 each component at the required concentration (Bradley et al., 2016). The large RSF1010 vector  
573 is able to replicate in a broad range of microbes including gram-negative bacteria such as *E.*

574 *coli* and several cyanobacterial species. However, for 25 years it has remained the only non-  
575 native vector reported to be able to self-replicate in cyanobacteria (Mermet-Bouvier et al.,  
576 1993). Recently, two small plasmids native to *Synechocystis*, pCA2.4 and pCB2.4, have been  
577 engineered for gene expression (Armshaw et al., 2015; Ng et al., 2015; Liu and Pakrasi, 2018).  
578 The pANS plasmid (native to PCC 7942) has also been adapted as a replicative vector, but so  
579 far it has been only shown to function in PCC 7942 and *Anabaena* PCC 7120 (Chen et al.,  
580 2016). Similarly, the high copy number plasmid pAQ1 (native to PCC 7002) has been  
581 engineered for heterologous expression, but up to now it has only been used in PCC 7002 (Xu  
582 et al., 2011). To expand the replication origins available for cyanobacterial research further we  
583 tested the capacity for vectors from the SEVA library to replicate in *Synechocystis* (Silva-  
584 Rocha et al., 2013).

585

586 We acquired three vectors driven by three different replication origins [pSEVA421 (RK2),  
587 pSEVA431 (pBBR1) and pSEVA442 (pRO1600/ColE1)] and carrying a spectinomycin  
588 antibiotic resistance marker. These vectors were domesticated and modified as level T acceptor  
589 vectors, assembled and then transformed into *Synechocystis* by electroporation or conjugation.  
590 Only *Synechocystis* strains conjugated with vectors carrying RK2 (pSEVA421-T) grew on  
591 spectinomycin-containing plates (**Supplementary Table S1; Supplementary Information**  
592 **S1**). To confirm that RSF1010 and RK2 replication origins can replicate autonomously in  
593 *Synechocystis*, we recovered the pPMQAK1-T or pSEVA421-T vector from lysates of axenic  
594 *Synechocystis* strains previously conjugated with each vector by transformation into *E. coli*.  
595 The identity and integrity of pPMQAK1-T and pSEVA421-T extracted from transformed *E.*  
596 *coli* colonies were confirmed by restriction digest and Sanger sequencing.

597

598 We then assembled two level T vectors with an eYFP expression cassette ( $P_{cpc560}$ -eYFP-  $T_{rrnB}$ )  
599 to produce pPMQAK1-T-eYFP and pSEVA421-T-eYFP, which were conjugated into  
600 *Synechocystis* (**Fig. 8; Supplementary Table S2**). Both pPMQAK1-T-eYFP and pSEVA421-  
601 T-eYFP transconjugates grew at similar rates in 50  $\mu\text{g ml}^{-1}$  kanamycin and 5  $\mu\text{g ml}^{-1}$   
602 spectinomycin, respectively (**Fig. 8A**). However, eYFP levels were 8-fold lower in  
603 pSEVA421-T-eYFP, suggesting that RK2 has a reduced copy number relative to RSF1010 in  
604 *Synechocystis* (**Fig. 8B**). We measured the heterologous plasmid vector copy number in strains  
605 expressing pSEVA421-T or pPMQAK1-T and estimated an average copy number per cell of  $9$   
606  $\pm 2$  and  $31 \pm 5$ , respectively (**Fig. 8C**). The copy number for pPMQAK1-T was similar to  
607 values reported previously for RSF1010-derived vectors in *Synechocystis* (ca. 30) (Ng et al.,

608 2000). Our results are also consistent with the lower copy numbers in *E. coli* for vectors with  
609 RK2 (4-7 copies) compared to RSF1010 (10-12 copies) replication origins (Frey et al., 1992;  
610 Blasina et al., 1996). Furthermore, we compared the genome copies per cell between  
611 transformants and wild-type strains and found no significant differences - the average value  
612 was  $11 \pm 2$ , which is consistent with the typical range of genome copy numbers observed in  
613 *Synechocystis* cells (Zerulla et al., 2016).

614

### 615 **Gene repression systems**

616 CRISPR (clustered regularly interspaced short palindromic) interference (CRISPRi) is a  
617 relatively new but well characterised tool for modulating genes expression at the transcription  
618 stage in a sequence-specific manner (Qi et al., 2013; Behler et al., 2018). CRISPRi typically  
619 uses a nuclease deficient Cas9 from *Streptococcus pyogenes* (dCas9) and has been  
620 demonstrated to work in several cyanobacterial species, including *Synechocystis* (Yao et al.,  
621 2015), PCC 7002 (Gordon et al., 2016); PCC 7942 (Huang et al., 2016) and *Anabaena* sp. PCC  
622 7120 (Higo et al., 2018). A second approach for gene repression uses rationally designed small  
623 regulatory RNAs (srRNAs) to regulate gene expression at the translation stage (Na et al., 2013;  
624 Higo et al., 2016). The synthetic srRNA is attached to a scaffold to recruit the Hfq protein, an  
625 RNA chaperone that is conserved in a wide-range of bacteria and cyanobacteria, which  
626 facilitates the hybridization of srRNA and target mRNA, and directs mRNA for degradation.  
627 The role of cyanobacterial Hfq in interacting with synthetic srRNAs is still unclear (Zess et al.,  
628 2016). However, regulatory ability can be improved by introducing Hfq from *E. coli* into  
629 *Synechocystis* (Sakai et al., 2015). Both CRISPRi- and srRNA-based systems have potential  
630 advantages as they can be used to repress multiple genes simultaneously.

631

632 To validate the CRISPRi system, we assembled an expression cassette for dCas9 ( $P_{cpc560}$ -  
633 dCas9- $T_{rrmB}$ ) on the Level 1 position 1 vector pICH47732, and four different sgRNA expression  
634 cassettes ( $P_{trc10\_TSS}$ -sgRNA-sgRNA scaffold) targeting eYFP on the Level 1 position 2 vector  
635 pICH47742 (Engler et al., 2014) (**Supplementary Table S2**). For assembly of CRISPRi  
636 sgRNA expression cassettes in level 1, we targeted four 18-22 bp regions of the eYFP non-  
637 template strand with an adjacent 3' protospacer adjacent motif (PAM) of 5'-NGG-3', as  
638 required by *S. pyogenes* dCas9 (**Fig. 9A**). The sgRNA sequences contained no off-target sites  
639 in the *Synechocystis* genome (confirmed by CasOT; Xiao et al., 2014). The sgRNAs were made  
640 by PCR using two complementary primers carrying the required overhangs and *BsaI* sites, and  
641 were assembled with  $P_{trc10\_TSS}$  promoter (pC0.203) and the sgRNA scaffold (pC0.122) (**Fig.**

642 **1K**). Level T vectors were assembled carrying dCas9 and a single sgRNA, or just the sgRNA  
643 alone. We subsequently conjugated the Olive-eYFP mutant and tracked eYFP expression.

644

645 Transconjugates carrying only the sgRNA showed no reduction in eYFP level compared to  
646 non-transconjugated Olive-eYFP (**Fig. 9B**). However, all strains carrying dCas9 and a sgRNA  
647 showed a decrease in eYFP that ranged from 40-90% depending on the sgRNA used. These  
648 reductions are similar to those observed previously in PCC 7002 and in *Synechocystis* (Yao et  
649 al., 2016; Gordon et al., 2016) and demonstrated that CRISPRi system is functional in the  
650 CyanoGate kit.

651

## 652 **CONCLUSION**

653 The CyanoGate kit was designed to increase the availability of well characterised libraries and  
654 standardised modular parts in cyanobacteria (Sun et al., 2018). We aimed to simplify and  
655 accelerate modular cloning methods in cyanobacterial research and allow integration with the  
656 growing number of labs that rely on the established common plant and algal syntax for multi-  
657 part DNA assembly (Patron et al., 2015; Crozet et al., 2018). Here, we have demonstrated the  
658 functionality of CyanoGate in sufficient detail to show that it is straightforward to adopt and  
659 functionally robust across two different cyanobacterial species. CyanoGate includes parts for  
660 usage in other cyanobacterial species and could likely be utilised also in non-cyanobacterial  
661 microbes amenable to transformation (e.g. *Rhodospseudomonas* spp.) and adapted for use in  
662 subcellular eukaryotic compartments of prokaryote origin (e.g. chloroplasts) (Economou et al.,  
663 2014; Doud et al., 2017; Leonard et al., 2018). In addition to the parts discussed, we have also  
664 assembled a suite of 21 terminators (**Supplementary Table S1**). To increase the accessibility  
665 and usability of the CyanoGate, we have included the vector maps for all parts and new  
666 acceptors (**Supplementary Information S1**), implemented support for Cyanogate assemblies  
667 in the online DNA “Design and Build” portal of the Edinburgh Genome Foundry  
668 ([dab.genomefoundry.org](http://dab.genomefoundry.org)) (**Supplementary Information S6**), and submitted all vectors as a  
669 toolkit for order from Addgene (Addgene Kit #1000000146;  
670 [www.addgene.org/kits/mccormick-cyanogate](http://www.addgene.org/kits/mccormick-cyanogate)).

671

672 Standardisation will help to accelerate the development of reliable synthetic biology tools for  
673 biotechnological applications and promote sharing and evaluation of genetic parts in different  
674 species and under different culturing conditions (Patron et al., 2015). Going forward, it will be  
675 important to test the performance of different parts with different components (e.g. gene

676 expression cassettes) and in different assembly combinations. Several groups using plant  
677 MoClo assembly have reported differences in cassette expression and functionality depending  
678 on position and orientations (e.g. Ordon et al., 2017), which highlights a key synthetic biology  
679 crux - the performance of a system is not simply the sum of its components (Mutalik et al.,  
680 2013; Heyduk et al., 2018).

681

682 The increasing availability of genome-scale metabolic models for different cyanobacterial  
683 species and their utilisation for guiding engineering strategies for producing heterologous high-  
684 value biochemicals has helped to re-invigorate interest in the industrial potential of  
685 cyanobacteria (Knoop et al., 2013; Hendry et al., 2016; Mohammadi et al., 2016; Shirai et al.,  
686 2016). Future efforts should focus on combining genome-scale metabolic models with  
687 synthetic biology approaches, which may help to overcome the production yield limitations  
688 observed for cyanobacterial cell factories (Nielsen et al., 2016), and will accelerate the  
689 development of more complex and precise gene control circuit systems that can better integrate  
690 with host metabolism and generate more robust strains (Bradley and Wang 2015; Jusiak et al.,  
691 2016; Luan and Lu, 2018). The future development of truly 'programmable' photosynthetic  
692 cells could provide significant advancements in addressing fundamental biological questions  
693 and tackling global challenges, including health and food security (Dobrin et al., 2016;  
694 Medford and Prasad, 2016; Smanksi et al., 2016).

695

## 696 **SUPPLEMENTARY DATA**

697 **Supplementary Table S1. Table of all parts from CyanoGate kit generated in this work.**

698 Domestication refers to the removal of *BsaI* and/or *BsiI* sites (modifications are indicated in  
699 sequence maps provided in **Supp. Info. 2**). See separate .xlsx.

700

701 **Supplementary Table S2. List of level T vectors used in this study.**

702

703 **Supplementary Table S3. Sequences of synthetic oligonucleotides used to determine copy  
704 number.** Primers used for amplifying the *petB* locus were from Pinto et al. (2012).

705

706 **Supplementary Information S1. Sequence maps (.gb files) of the components of the  
707 CyanoGate kit.** See .zip file.

708

709 **Supplementary Information S2. Protocols for MoClo assembly in level -1 through to level**  
710 **T.** Protocols for assembly in level 0, level M and level T acceptor vectors (restriction enzyme  
711 *BpiI* required, left). Protocols for assembly in level -1, level 1 and level P backbone vectors  
712 (restriction enzyme *BsaI* required, right). Adapted from “A quick guide to Type IIS cloning”  
713 (Patron Lab; [patronlab.org](http://patronlab.org)). For troubleshooting Type IIS mediated assembly we recommend  
714 [synbio.tsl.ac.uk/docs](http://synbio.tsl.ac.uk/docs).

715

716 **Supplementary Information S3. Detailed assembly strategies using the CyanoGate kit.**

717

718 **Supplementary Information S4. Integrative engineering strategies using the CyanoGate**

719 **kit.** (A) Marked mutants are generated using a level T marked knock out vector carrying DNA  
720 sequences flanking the target locus of the chromosome (~1 kb), an antibiotic resistance cassette  
721 ( $Ab^R$ ) and a sucrose selection cassette (*sacB*) that produces the toxic compound levansucrase  
722 in the presence of sucrose (20). Several rounds of segregation are required to identify a marked  
723 mutant. (B) Marked mutants then can be unmarked with a level T unmarked knock out vector  
724 and selection on sucrose-containing agar plates. (C) Unmarked knock in mutants can also be  
725 generated from marked mutants using a level T unmarked knock in vector carrying a gene  
726 expression cassette (UP FLANK LINKER and DOWN FLANK LINKER are shown in pink  
727 and light green, respectively). (D) Alternatively marked knock in mutants can be engineered in  
728 a single step using a level T marked knock vector ( $Ab^R$  UP LINKER and DOWN LINKER are  
729 shown in blue and orange, respectively). See **Fig. 2** for abbreviations.

730

731 **Supplementary Information S5. Comparison of Gibson Assembly and Golden Gate**

732 **Assembly.** (A) A comparison of Gibson Assembly and Golden Gate Assembly pathways for  
733 building the level T vector *cpcBA-eYFP* described in **Fig. 4**. (B) Advantages and disadvantages  
734 of Gibson Assembly and Golden Gate Assembly.

735

736 **Supplementary Information S6. Protocol and online interface for building CyanoGate**

737 **vector assemblies.** A CyanoGate online vector assembly tool called Design and Build (DAB)  
738 from the Edinburgh Genome Foundry.

739

740 **Supplementary Figure S1. Comparison of growth for *Synechocystis*, PCC 7942 and**

741 **UTEX 2973 under different culturing conditions.** Values are the means  $\pm$  SE from at least  
742 five biological replicates from two independent experiments.

743

744 **Supplementary Figure S2. Growth and expression levels of heterologous and synthetic**  
745 **promoters in *Synechocystis* and UTEX 2973.** (A) *Synechocystis* and UTEX 2973 was  
746 cultured for 72 hr at 30°C with continuous light (100  $\mu\text{mol photons m}^{-2} \text{s}^{-1}$ ) and 40°C with 300  
747  $\mu\text{mol photons m}^{-2} \text{s}^{-1}$ , respectively (see **Fig. 6**). Expression levels of eYFP are shown at three  
748 time points (24, 48 and 72 hr after inoculation). Values are the means  $\pm$  SE from at least four  
749 biological replicates where each replicate represents the median measurements of 10,000 cells.  
750

751 **Supplementary Figure S3. Cell volume calculations for *Synechocystis* and UTEX 2973**  
752 **from confocal microscopy images.** (A) Example confocal images of *Synechocystis* (left) and  
753 UTEX 2973 (right) cells expressing eYFP driven by the J23119 promoter at 48 hr. Individual  
754 cells were selected and measured using Leica AF Lite software (Leica Microsystems). Top  
755 panel: eYFP fluorescence (green); middle panel: chlorophyll auto fluorescence (red); bottom  
756 panel: overlay of eYFP and chlorophyll signals (yellow). (B) Volume estimations based on  
757 confocal image data (n =50) (C) Mathematical formulas used for calculating cell volume based  
758 on the cell shapes of *Synechocystis* (coccus, spherical) and UTEX 2973 (bacillus, cylindrical).  
759

## 760 **ACKNOWLEDGEMENTS**

761 We thank Conrad Mullineaux (Queen Mary University), Julie Zedler and Poul Erik Jensen  
762 (University of Copenhagen) for providing components for conjugation, and Eva Steel  
763 (University of Edinburgh) for assistance with assembling the CyanoGate kit. RV, AJM, BW  
764 and CJH were funded by the PHYCONET Biotechnology and Biological Sciences Research  
765 Council (BBSRC) Network in Industrial Biotechnology and Bioenergy (NIBB) and the  
766 Industrial Biotechnology Innovation Centre (IBioIC). GARG was funded by a BBSRC  
767 EASTBIO CASE PhD studentship (grant number BB/M010996/1). BW acknowledges funding  
768 support by UK BBSRC grant (BB/N007212/1) and Leverhulme Trust research grant (RPG-  
769 2015-445). AAS was funded by a Consejo Nacional de Ciencia y Tecnología (CONACYT)  
770 PhD studentship. KV was supported by a CSIRO Synthetic Biology Future Science Fellowship.



## FIGURE LEGENDS

**Figure 1. Adaptation of the Plant Golden Gate MoClo level 0 syntax for generating level 1 assemblies for transfer to Level T.** (A) The format for a level 0 MoClo acceptor vector with the part bordered by two *BsaI* sites. (B) Typical level 0 parts from the Plant MoClo kit (38), where parts of the same type are bordered by the same pair of fusion sites (for each fusion site, only the sequence of the top strand is shown). Note that the parts are not drawn to scale. (C, D) The syntax of the Plant MoClo kit was adapted to generate level 0 parts for engineering marked and unmarked cyanobacterial mutant strains (20). (E-I) To generate knock in mutants, short linker parts (30 bp) were constructed to allow assembly of individual flanking sequences, or marker cassettes (*Ab<sup>R</sup>* or *sacB*) in level 1 vectors for subsequent assembly in level T. (J, K) Parts required for generating synthetic srRNA or CRISPRi level 1 constructs. See **Supplementary Information S3 and S4** for workflows. Abbreviations: 3U+Ter, 3'UTR and terminator; *Ab<sup>R</sup>*, antibiotic resistance cassette; *Ab<sup>R</sup>* DOWN LINKER, short sequence (~30 bp) to provide CGCT overhang; *Ab<sup>R</sup>* UP LINKER, short sequence (~30 bp) to provide GAGG overhang; CDS2(stop), coding sequence with a stop codon; DOWN FLANK, flanking sequence downstream of target site; DOWN FLANK LINKER, short sequence (~30 bp) to provide GGAG overhang; Prom+5U, promoter and 5' UTR; Prom TSS, promoter transcription start site; *sacB*, levansucrase expression cassette; *sacB* UP LINKER, short sequence (~30 bp) to provide GAGG overhang; sgRNA, single guide RNA; SP, signal peptide; srRNA, small regulatory RNA; UP FLANK, flanking sequence upstream of target site; UP FLANK LINKER, short sequence (~30 bp) to provide CGCT overhang; UNMARK LINKER, short sequence to bridge UP FLANK and DOWN FLANK.

**Figure 2. Extension of the Plant Golden Gate MoClo Assembly Standard for cyanobacterial transformation.** Assembly relies on one of two Type IIS restriction endonuclease enzymes (*BsaI* or *BpiI*). Domesticated level 0 parts are assembled into level 1 vectors. Up to seven level 1 modules can be assembled directly into a level T cyanobacterial transformation vector, which consist of two sub-types (either a replicative or an integrative vector). Alternatively, larger vectors with more modules can be built by assembling level 1 modules into level M, and then cycling assembly between level M and level P, and finally transferred from Level P to level T. Antibiotic selection markers are shown for each level. Level T vectors are supplied with internal antibiotic selection markers (shown), but additional selection markers could be included from level 1 modules as required. See **Supplementary Table S1 and Supplementary Information S1** for full list and maps of level T acceptor vectors.

**Figure 3. Generating knock out mutants in cyanobacteria.** (A) Assembled level T vector *cpcBA*-M (see Fig. 1C) targeting the *cpcBA* promoter and operon (3,563 bp) to generate a marked  $\Delta cpcBA$  “Olive” mutant in *Synechocystis* sp. PCC 6803. Following transformation and segregation on kanamycin (*ca.* 3 months), a segregated marked mutant was isolated (WT band is 3,925 bp, marked mutant band is 5,503 bp, 1kb DNA ladder (NEB) is shown). (B) Assembled level T vector *cpcBA*-UM (see Fig. 1D) for generating an unmarked  $\Delta cpcBA$  mutant. Following transformation and segregation on sucrose (*ca.* 2 weeks), an unmarked mutant was isolated (unmarked band is 425 bp). (C) Liquid cultures of WT, marked and unmarked Olive mutants. (D) Spectrum showing the absorbance of the unmarked Olive mutant and WT cultures after 72 hr of growth. Values are the average of four biological replicates  $\pm$  SE and are standardised to 750 nm.

**Figure 4. Generating knock in mutants in cyanobacteria.** (A) Assembly of level 1 modules *cpcBA*-UF (see Fig. 1E) in the level 1, position 1 acceptor (L1P1),  $P_{cpc560}$ -eYFP-*T<sub>rrmB</sub>* (see Fig. 1G) in L1P2 and *cpcBA*-DF (see Fig. 1F) in L1P3. (B) Transfer of level 1 assemblies to level T vector *cpcBA*-eYFP for generating an unmarked  $\Delta cpcBA$  mutant carrying an eYFP expression cassette. Following transformation and segregation on sucrose (*ca.* 3 weeks), an unmarked eYFP mutant was isolated (1,771 bp). (C) Fluorescence values are the means  $\pm$  SE of four biological replicates, where each replicate represents the median measurements of 10,000 cells.

**Figure 5. Expression levels of cyanobacterial promoters in *Synechocystis* and UTEX 2973.** (A) Structure of the cyanobacterial promoters adapted for the CyanoGate kit. Regions of  $P_{cpc560}$  shown are the upstream transcription factor binding sites (TFBSs) (-556 to -381 bp), middle region (-380 to -181 bp), and the downstream TFBSs, ribosome binding site (RBS) and spacer (-180 to -5 bp) (B) Expression levels of eYFP driven by promoters in *Synechocystis* and UTEX 2973 calculated from measurements taken from 10,000 individual cells. Values are the means  $\pm$  SE from at least four biological replicates after 48 hr of growth (average OD<sub>750</sub> values for *Synechocystis* and UTEX 2973 cultures were  $3.5 \pm 0.2$  and  $3.6 \pm 0.2$ , respectively). See **Supplementary Figure S2** for more info.

**Figure 6. Expression levels of heterologous and synthetic promoters in *Synechocystis* and UTEX 2973.** (A) Structure and alignment of eight new synthetic promoters derived from the

BioBricks BBa\_J23119 library and  $P_{trc10}$  promoter design (18). (B) Expression levels of eYFP driven by promoters in *Synechocystis* and UTEX 2973 calculated from measurements taken from 10,000 individual cells. (C) Correlation analysis of expression levels of synthetic promoters tested in *Synechocystis* and UTEX 2973. The coefficient of determination ( $R^2$ ) is shown for the J23119 library (red), new synthetic promoters (pink) and *trc* variants (dark red). Values are the means  $\pm$  SE from at least four biological replicates after 48 hr of growth (average  $OD_{750}$  values for *Synechocystis* and UTEX 2973 cultures were  $3.5 \pm 0.2$  and  $3.6 \pm 0.2$ , respectively). See **Supplementary Figure S2** for more info.

**Figure 7. Protein expression levels in *Synechocystis* and UTEX 2973 cells.** (A) Confocal images of WT strains and mutants expressing eYFP (fluorescence shown in yellow) driven by the J23119 promoter (bar = 10  $\mu$ m). (B) Representative immunoblot of protein extracts (3  $\mu$ g protein) from mutants with different promoter expression cassettes (as in **Fig. 6**) probed with an antibody against eYFP. The protein ladder band corresponds to 30 kDa. (E) Relative eYFP protein abundance relative to UTEX 2973 mutants carrying the J23119 expression cassette. (C-E) Cell density, protein content per cell and protein density per estimated cell volume for *Synechocystis* and UTEX 2973. Asterisks (\*) indicate significant difference ( $P < 0.05$ ) as determined by Student's *t*-tests. Values are the means  $\pm$  SE of four biological replicates.

**Figure 8. Growth and expression levels of eYFP with the RK2 replicative origin in *Synechocystis*.** (A) Growth of strains carrying RK2 (vector pSEVA421-T-eYFP), RSF1010 (pPMQAK1-T-eYFP) or an empty pPMQAK1-T grown in appropriate antibiotics. Growth was measured as  $OD_{750}$  under a constant illumination of 100  $\mu$ mol photons  $m^{-2}s^{-1}$  at 30 °C. (B) Expression levels of eYFP after 48 hr of growth calculated from measurements taken from 10,000 individual cells. (C) Plasmid copy numbers per cell after 48 hr of growth. Letters indicating significant difference ( $P < 0.05$ ) are shown, as determined by ANOVA followed by Tukey's HSD tests. Values are the means  $\pm$  SE of four biological replicates.

**Figure 9. Gene regulation system using CRISPRi in *Synechocystis*.** (A) Four target regions were chosen as sgRNA protospacers to repress eYFP expression in Olive-eYFP (**Fig. 4**): 'CCAGGATGGGCACCACCC' (+31), 'ACTTCAGGGTCAGCTTGCCGT' (+118), 'AGGTGGTCACGAGGGTGGGCCA' (+171) and 'AGAAGTCGTGCTGCTTCATG' (+233). (B) eYFP fluorescence of Olive-eYFP expressing constructs carrying sgRNAs with and without dCas9 (representative of 10,000 individual cells). Untransformed Olive-eYFP and

the Olive mutant were used as controls. Letters indicating significant difference ( $P < 0.05$ ) are shown, as determined by ANOVA followed by Tukey's HSD tests. Values are the means  $\pm$  SE of four biological replicates.

## REFERENCES

- Abe, K., Sakai, Y., Nakashima, S., Araki, M., Yoshida, W., Sode, K., Ikebukuro, K. (2014) Design of riboregulators for control of cyanobacterial (*Synechocystis*) protein expression. *Biotechnol. Lett.*, **36**, 287–294.
- Albers, S.C., Gallegos, V.A., Peebles, C.A.M. (2015) Engineering of genetic control tools in *Synechocystis* sp. PCC 6803 using rational design techniques. *J. Biotechnol.*, **216**, 36–46.
- Andersson, C.R., Tsinoremas, N.F., Shelton, J., Lebedeva, N.V., Yarrow, J., Min, H., Golden, S.S. (2000) Application of bioluminescence to the study of circadian rhythms in cyanobacteria. *Methods Enzymol.*, **305**, 527–542.
- Andreou, A.I., Nakayama, N. (2018) Mobius Assembly: A versatile Golden-Gate framework towards universal DNA assembly. *PLoS ONE*, **13**, e0189892.
- Armshaw, P., Carey, D., Sheahan, C., Pembroke, J.T. (2015) Utilising the native plasmid, pCA2.4, from the cyanobacterium *Synechocystis* sp. strain PCC6803 as a cloning site for enhanced product production. *Biotechnol. Biofuels* **8**, 201.
- Behler, J., Vijay, D., Hess, W.R., Akhtar, M.K. (2018) CRISPR-based technologies for metabolic engineering in cyanobacteria. *Trends Biotechnol.*, pii: S0167-7799(18)30146-X.
- Bhal, C.P., Wu, R., Stawinsky, J., Narang, S.A. (1977) Minimal length of the lactose operator sequence for the specific recognition by the lactose repressor. *Proc. Natl. Acad. Sci. U.S.A.*, **74**, 966–970.
- Blasi, B., Peca, L., Vass, I., Kós, P.B. (2012) Characterization of stress responses of heavy metal and metalloinducible promoters in *Synechocystis* PCC6803. *J. Microbiol. Biotechnol.*, **22**, 166–169.
- Blasina, A., Kittell, B.L., Toukdarian, A.E., Helinski, D.R. (1996) Copy-up mutants of the plasmid RK2 replication initiation protein are defective in coupling RK2 replication origins. *Proc. Natl. Acad. Sci. U.S.A.*, **93**, 3559–3564.
- Bradley, R.W., Buck, M., Wang, B. (2016) Tools and principles for microbial gene circuit engineering. *J. Mol. Biol.*, **428**, 862–882.
- Bradley, R.W., Wang, B. (2015) Designer cell signal processing circuits for biotechnology. *N. Biotechnol.*, **32**, 635–643.
- Bustos S.A., Golden, S.S. (1992) Light-regulated expression of the PsbD gene family in *Synechococcus* sp. strain PCC 7942: evidence for the role of duplicated PsbD genes in cyanobacteria. *Mol. Gen. Genet.*, **232**, 221–230.
- Castenholz, R.W. (2001) Phylum BX. Cyanobacteria. Oxygenic photosynthetic bacteria. In: Garrity, G., Boone, D.R., Castenholz, R.W. (eds) *Bergey's manual of systematic bacteriology*. Springer, New York, pp 473–599.
- Camsund, D., Heidorn, T., and Lindblad, P. (2014) Design and analysis of LacI-repressed promoters and DNA-looping in a cyanobacterium. *J. Biol. Eng.*, **8**, e4.
- Chambers, S., Kitney, R., Freemont, P. (2016) The Foundry: the DNA synthesis and construction Foundry at Imperial College. *Biochem. Soc. Trans.*, **44**, 687–688.
- Chen, Y., Taton, A., Go, M., London, R.E., Pieper, L.M., Golden, S.S., Golden, J.W. (2016). Self-replicating shuttle vectors based on pANS, a small endogenous plasmid of the unicellular cyanobacterium *Synechococcus elongatus* PCC 7942. *Microbiology*, **162**, 2029–2041.

- Clerico, E.M., Ditty, J.L., Golden, S.S. (2007) Specialized techniques for site-directed mutagenesis in cyanobacteria. *Methods Mol. Biol.*, **362**, 155–171.
- Crozet, P., Navarro, F.J., Willmund, F., Mehrshahi, P., Bakowski, K., Lauersen, K.J., Pérez-Pérez, M.E., Auroy, P., Gorchs Rovira, A., Sauret-Gueto, S., Niemeyer, J., Spaniol, B., Theis, J., Trösch, R., Westrich, L.D., Vavitsas, K., Baier, T., Hübner, W., de Carpentier, F., Cassarini, M., Danon, A., Henri, J., Marchand, C.H., de Mia, M., Sarkissian, K., Baulcombe, D.C., Peltier, G., Crespo, J.L., Kruse, O., Jensen, P.E., Schroda, M., Smith, A.G., Lemaire, S.D. (2018) Birth of a photosynthetic chassis: A MoClo toolkit enabling synthetic biology in the microalga *Chlamydomonas reinhardtii*. *ACS Synth. Biol.*, **7**, 2074–2086.
- Dexter, J., Dziga, D., Lv, J., Zhu, J., Strzalka, W., Maksylewicz, A., Maroszek, M., Marek, S., Fu, P. (2018). Heterologous expression of mlrA in a photoautotrophic host – Engineering cyanobacteria to degrade microcystins. *Environ. Pollut.*, **237**, 926–935.
- Dobrin, A., Saxena, P., Fussenegger, M. (2016) Synthetic biology: applying biological circuits beyond novel therapies. *Integr. Biol.*, **8**, 409–430.
- Doud, D.F.R., Holmes, E.C., Richter, H., Molitor, B., Jander, G., Angenent, L.T. (2017) Metabolic engineering of *Rhodospseudomonas palustris* for the obligate reduction of n-butyrate to n-butanol. *Biotechnol. Biofuels.*, **10**, 178.
- Ducat, D.C., Way, J.C., Silver, P.A. (2010) Engineering cyanobacteria to generate high-value products. *Trends Biotechnol.*, **29**, 95–103.
- Economou, C., Wannathong, T., Szaub, J., Purton, S. (2014) A simple, low-cost method for chloroplast transformation of the green alga *Chlamydomonas reinhardtii*. *Methods Mol. Biol.*, **1132**, 401–411.
- Engler, C., Youles, M., Gruetzner, R., Ehnert, T-M., Werner, S., Jones, J.D.G., Patron, N.J., Marillonnet, S. (2014) A Golden Gate modular cloning toolbox for plants. *ACS Synth. Biol.*, **3**, 839–843.
- Englund, E., Liang, F., Lindberg, P. (2016) Evaluation of promoters and ribosome binding sites for biotechnological applications in the unicellular cyanobacterium *Synechocystis* sp. PCC 6803. *Sci. Rep.*, **6**, A36640.
- Ferreira, E.A., Pacheco, C.C., Pinot, F., Pereira, J., Lamosa, P., Oliveira, P., Kirov, B., Jaramillo, A., Tamagnini, P. (2018) Expanding the toolbox for *Synechocystis* sp. PCC 6803: validation of replicative vectors and characterization of a novel set of promoters. *Synth. Biol.*, **3**, ysy014.
- Flombaum, P., Gallegos, J.L., Gordillo, R.A., Rincón, J., Zabala, L.L., Jiao, N., Karl, D.M., Li, W.K.W., Lomas, M.W., Veneziano, D., Vera, C.S., Vrugt, J.A., Martiny, A.C. (2013) Present and future global distributions of the marine Cyanobacteria *Prochlorococcus* and *Synechococcus*. *Proc. Natl. Acad. Sci. U.S.A.*, **110**, 9824–9829.
- Frey, J., Bagdasarian, M.M., Bagdasarian, M. (1992) Replication and copy number control of the broad-host-range plasmid RSF1010. *Gene*, **113**, 101–106.
- Gao, X., Gao, F., Liu, D., Zhang, H., Nie, X., Yang, C. (2016) Engineering the methylerythritol phosphate pathway in cyanobacteria for photosynthetic isoprene production from CO<sub>2</sub>. *Energy Environ. Sci.*, **9**, 1400–1411.
- Gibson, D.G., Young, L., Chuang, R.Y., Venter, J.C., Hutchison C.A., Smith, H.O. (2009) Enzymatic assembly of DNA molecules up to several hundred kilobases. *Nat. Methods*, **6**, 343–345.
- Gordon, G.C., Korosh, T.C., Cameron, J.C., Markley, A.L., Begemann, M.B., Pfleger, B.F. (2016) CRISPR interference as a titratable, trans-acting regulatory tool for metabolic engineering in the cyanobacterium *Synechococcus* sp. strain PCC 7002. *Metab. Eng.*, **38**, 170–179.

- Guerrero, F., Carbonell, V., Cossu, M., Correddu, D., Jones, P.R. (2012) Ethylene synthesis and regulated expression of recombinant protein in *Synechocystis* sp. PCC 6803. *PLoS ONE*, **7**, e50470.
- Immethun, C.M., DeLorenzo, D.M., Focht, C.M., Gupta, D., Johnson, C.B., Moon, T.S. (2017) Physical, chemical, and metabolic state sensors expand the synthetic biology toolbox for *Synechocystis* sp. PCC 6803. *Biotechnol Bioeng.*, **114**, 1561–1569.
- Heidorn, T., Camsund, D., Huang, H., Lindberg, P., Oliveira, P., Stensjö, K., Lindblad, P. (2011) Synthetic biology in cyanobacteria engineering and analyzing novel functions. *Methods Enzymol.*, **497**, 539–579.
- Hendry, J.I., Prasannan, C.B., Joshi, A., Dasgupta, S., Wangikar, P.P. (2016) Metabolic model of *Synechococcus* sp. PCC 7002: Prediction of flux distribution and network modification for enhanced biofuel production. *Bioresour Technol.*, **213**, 190–197.
- Heyduk, E., Heyduk, T. (2018) DNA template sequence control of bacterial RNA polymerase escape from the promoter. *Nucleic Acids Res.*, **46**, 4469–4486.
- Higo, A., Isu, A., Fukaya, Y., Ehira, S., Hisabori, T. (2018) Application of CRISPR interference for metabolic engineering of the heterocyst-forming multicellular cyanobacterium *Anabaena* sp. PCC 7120. *Plant Cell Physiol.*, **59**, 119–127.
- Higo, A., Isu, A., Fukaya, Y., Hisabori, T. (2016) Efficient gene induction and endogenous gene repression systems for the filamentous cyanobacterium *Anabaena* sp. PCC 7120.
- Huang, C.H., Shen, C.R., Li, H., Sung, L.Y., Wu, M.Y., Hu, Y.C. (2016) CRISPR interference (CRISPRi) for gene regulation and succinate production in cyanobacterium *S. elongatus* PCC 7942. *Microb. Cell Fact.*, **15**, 196.
- Huang, H., Camsund, D., Lindblad, P., Heidorn, T. (2010) Design and characterization of molecular tools for a Synthetic Biology approach towards developing cyanobacterial biotechnology. *Nucleic Acids Res.*, **38**, 2577–2593.
- Huang, H., Lindblad, P. (2013) Wide-dynamic-range promoters engineered for cyanobacteria. *J. Biol. Eng.*, **7**, 10.
- Jusiak, B., Cleto, S., Perez-Piñera, P., Lu, T.K. (2016) Engineering synthetic gene circuits in living cells with CRISPR technology. *Trends Biotechnol.*, **34**, 535–547.
- Keeling, P.J. (2003) Diversity and evolutionary history of plastids and their hosts. *Am. J. Bot.*, **10**, 1481–1493.
- Kelly, C.L., Hitchcock, A., Torres-Méndez, A., Heap, J.T. (2018) A rhamnose-inducible system for precise and temporal control of gene expression in cyanobacteria. *ACS Synth. Biol.*, **7**, 1056–1066.
- Kikuchi, H., Aichi, M., Suzuki, I., Omato, T. (1996) Positive regulation by nitrite of the nitrate assimilation operon in the cyanobacteria *Synechococcus* sp. strain PCC 7942 and *Plectonema boryanum*. *J. Bacteriol.*, **178**, 5822–5825.
- Kim, W.J., Lee, S.M., Um, Y., Sim, S.J., Woo, H.M. (2017) Development of SyneBrick vectors as a synthetic biology platform for gene expression in *Synechococcus elongatus* PCC 7942. *Front. Plant Sci.*, **8**, A293.
- Kirst, H., Formighieri, C., Melis, A. (2014) Maximizing photosynthetic efficiency and culture productivity in cyanobacteria upon minimizing the phycobilisome light-harvesting antenna size. *Biochim. Biophys. Acta*, **1837**, 1653–1664.
- Knoop, H., Gründel, M., Zilliges, Y., Lehmann, R., Hoffmann, S., Lockau, W., Steuer, R. (2013) Flux Balance Analysis of Cyanobacterial Metabolism: The Metabolic Network of *Synechocystis* sp. PCC 6803. *PLoS Comput. Biol.*, **9**, e1003081.
- Kulkarni, D.R., Golden, S.S. (1997). mRNA stability is regulated by a coding-region element and the unique 5' untranslated leader sequences of the three *Synechococcus* psbA transcripts. *Mol. Microbiol.*, **24**, 1131–1142.

- Kunert, A., Vinnemeier, J., Erdmann, N., Hagemann, M. (2003) Repression by Fur is not the main mechanism controlling the iron-inducible *isiAB* operon in the cyanobacterium *Synechocystis* sp. PCC 6803. *FEMS Microbiol. Lett.*, **227**, 255–262.
- Lea-Smith, D.J., Bombelli, P., Dennis, J.S., Scott, S.A., Smith, A.G. Howe, C.J. (2014) Phycobilisome-deficient strains of *Synechocystis* sp. PCC 6803 have reduced size and require carbon-limiting conditions to exhibit enhanced productivity. *Plant Physiol.*, **165**, 705–714.
- Lea-Smith, D.J., Ross, N., Zori, M., Bendall, D.S., Dennis, J.S., Scott, S.A., Smith, A.G., Howe, C.J. (2013) Thylakoid terminal oxidases are essential for the cyanobacterium *Synechocystis* sp. PCC 6803 to survive rapidly changing light intensities. *Plant Physiol.*, **162**, 484–495.
- Lea-Smith, D.J., Vasudevan, R., Howe, C.J. (2016) Generation of marked and markerless mutants in model cyanobacterial species. *J. Vis. Exp.*, **111**, e54001.
- Leonard, S.P., Perutka, J., Powell, J.E., Geng, P., Richhart, D.D., Byrom, M., Kar, S., Davies, B.W., Ellington, A.D., Moran, N.A., Barrick, J.E. (2018) Genetic engineering of bee gut microbiome bacteria with a toolkit for modular assembly of broad-host-range plasmids. *ACS Synth. Biol.*, **7**, 1279–1290.
- Li, L., Jaing, W., Lu, Y. (2018) A modified Gibson Assembly method for cloning large DNA fragments with high GC contents. *Methods Mol. Biol.*, **1671**, 203–209.
- Li, S., Sun, T., Xu, C., Chen, L., Zhang, W. (2018) Development and optimization of genetic toolboxes for a fast-growing cyanobacterium *Synechococcus elongatus* UTEX 2973. *Metab. Eng.*, **48**, 163–174.
- Liberton, M., Chrisler, W.B., Nicora, C.D., Moore, R.J., Smith, R.D., Koppelaar, D.W., Pakrasi, H.B., Jacobs, J.M. (2017) Phycobilisome truncation causes widespread proteome changes in *Synechocystis* sp. PCC 6803. *PLoS ONE*, **12**, e0173251.
- Lindberg, P., Park, S., Melis, A. (2010) Engineering a platform for photosynthetic isoprene production in cyanobacteria, using *Synechocystis* as the model organism. *Metab. Eng.*, **12**, 70–79.
- Luan, G., Lu, X. (2018) Tailoring cyanobacterial cell factory for improved industrial properties. *Biotechnol. Adv.*, **36**, 430–442.
- Liu, Q., Schumacher, J., Wan, X., Lou, C., Wang, B. (2018) Orthogonality and burdens of heterologous AND Gate gene circuits in *E. coli*. *ACS Synth. Biol.*, **7**, 553–564.
- Liu, D., Pakrasi, B.H. (2018) Exploring native genetic elements as plug-in tools for synthetic biology in the cyanobacterium *Synechocystis* sp. PCC 6803. *Microb. Cell Fact.*, **17**, 48.
- Lou, W., Tan, X., Song, K., Zhang, S., Luan, G., Li, C., Lu, X. (2018) A specific single nucleotide polymorphism in the ATP synthase gene significantly improves environmental stress tolerance of *Synechococcus elongatus* PCC 7942. *Appl. Environ. Microbiol.*, **84**, e01222-18.
- Madsen, M.A., Semerdzhiev, S., Amtmann, A., Tonon, T. (2018) Engineering mannitol biosynthesis in *Escherichia coli* and *Synechococcus* sp. PCC 7002 using a green algal fusion protein. *ACS Synth. Biol.*, **7**, 2833–2840.
- Markley, A.L., Begemann, M.B., Clarke, R.E., Gordon, G.C., Pfluge, B.F. (2015) Synthetic biology toolbox for controlling gene expression in the cyanobacterium *Synechococcus* sp. strain PCC 7002. *ACS Synth Biol.*, **4**, 595–603.
- Marraccini, P., Bulteau, S., Cassier-Chauvat, C., Mermet-Bouvier, P., Chauvat, F. (1993) A conjugative plasmid vector for promoter analysis in several cyanobacteria of the genera *Synechococcus* and *Synechocystis*. *Plant Mol. Biol.*, **23**, 905–909.
- McCormick, A.J., Bombelli, P., Bradley, R.W., Thorne, R., Wenzel, T., Howe, C.J. (2015) Biophotovoltaics: oxygenic photosynthetic organisms in the world of bioelectrochemical systems. *Energy Environ. Sci.*, **8**, 1092–1109.

- Medford, J.I., Prasad, A. (2016) Towards programmable plant genetic circuits. *Plant J.*, **87**, 139–148.
- Mermet-Bouvier, P., Cassier-Chauvat, C., Marraccini, P., Chauvat, F. (1993) Transfer and replication of RSF1010-derived plasmids in several cyanobacteria of the general *Synechocystis* and *Synechococcus*. *Curr. Microbiol.* **27**, 323–327.
- Mohammadi, R., Fallah-Mehrabadi, J., Bidkhor, G., Zahiri, J., Javad Niroomand, M., Masoudi-Nejad, A. (2016) A systems biology approach to reconcile metabolic network models with application to *Synechocystis* sp. PCC 6803 for biofuel production. *Mol. Biosyst.*, **12**, 2552–2561.
- Moore, S.J., Lai, H-E., Kelwick, R.J.R., Chee, S.M., Bell, D.J., Polizzi, K.M., Freemont, P.S. (2016) EcoFlex: a multifunctional MoClo kit for *E. coli* synthetic biology. *ACS Synth. Biol.*, **5**, 1059–1069.
- Mueller, T.J., Ungerer, J.L., Pakrasi, H.B., Maranas, C.D. (2017) Identifying the metabolic differences of a fast-growth phenotype in *Synechococcus* UTEX 2973. *Sci. Rep.*, **7**, 41569.
- Munch, R., Hiller, K., Grote, A., Scheer, M., Klein, J., Schobert, M., Jahn, D. (2005) Genome analysis Virtual Footprint and PRODORIC: an integrative framework for regulon prediction in prokaryotes. *Bioinforma. Appl. Note* **21**, 4187–4189.
- Mutalik, V.K., Guimaraes, J.C., Cambray, G., Mai, Q.A., Christoffersen, M.J., Martin, L., Yu, A., Lam, C., Rodriguez, C., Bennett, G., Keasling, J.D., Endy, D., Arkin, A.P. (2013) Quantitative estimation of activity and quality for collections of functional genetic elements. *Nat. Methods* **10**, 347–353.
- Na, D., Yoo, S.M., Chung, H., Park, H., Park, J.H., Lee, S.Y. (2013) Metabolic engineering of *Escherichia coli* using synthetic small regulatory RNAs. *Nat. Biotechnol.*, **31**, 170–174.
- Niederholtmeyer, H., Wolfstädter, B.T., Savage, D.F., Silver, P.A., Way, J.C. (2010) Engineering cyanobacteria to synthesize and export hydrophilic products. *Appl. Environ. Microbiol.*, **76**, 3462–3466.
- Nielsen, A.Z., Mellor, S.B., Vavitsas, K., Włodarczyk, A.J., Gnanasekaran, T., de Jesus, M.P.R.H., King, B.C. Bakowski, K., Jensen, P.E. (2016) Extending the biosynthetic repertoires of cyanobacteria and chloroplasts. *Plant J.*, **87**, 87–102.
- Nielsen, J., Keasling, J.D. (2016) Engineering cellular metabolism. *Cell*, **164**, 1185–1197.
- Ng, A.H., Berla, B.M., Pakrasi, H.B. (2015) Fine-tuning of photoautotrophic protein production by combining promoters and neutral sites in the cyanobacterium *Synechocystis* sp. strain PCC 6803. *Appl. Environ. Microbiol.* **81**, 6857–6863.
- Ng, W.O., Zentella, R., Wang, Y., Taylor, J.S., Pakrasi, H.B. (2000) PhrA, the major photoreactivating factor in the cyanobacterium *Synechocystis* sp. strain PCC 6803 codes for a cyclobutane-pyrimidine-dimer-specific DNA photolyase. *Arch. Microbiol.*, **173**, 412–417.
- Ordon, J., Gantner, J., Kemna, J., Schwalgun, L., Reschke, M., Streubel, J., Boch, J., Stuttmann, J. (2017) Generation of chromosomal deletions in dicotyledonous plants employing a user-friendly genome editing toolkit. *Plant J.*, **89**:155–168.
- Patron, N.J., Orzaez, D., Marillonnet, S., Warzecha, H., Matthewman, C., Youles, M., Raitskin, O., Leveau, A., Farré, G., Rogers, C., Smith, A., Hibberd, J., Webb, A.A. *et al.* (2015) Standards for plant synthetic biology: a common syntax for exchange of DNA parts. *New Phytol.*, **208**, 13–19.
- Peca, L., Kós, P.B., Máté, Z., Farsang, A., Vass, I. (2008) Construction of bioluminescent cyanobacterial reporter strains for detection of nickel, cobalt and zinc. *FEMS Microbiol. Lett.*, **289**, 258–264.
- Pinto, F., Pacheco, C.,C., Ferreira, D., Moradas-Ferreira, P., Tamagnini, P. (2012) Selection of suitable reference genes for RT-qPCR analyses in cyanobacteria. *PLoS ONE*, **7**, e34983.
- Pinto, F., Pacheco, C.,C., Oliveira, P., Montagud, A., Landels, A., Couto, N., Wright, P.,C., Urchueguía, J.,F., Tamagnini, P. (2015) Improving a *Synechocystis*-based photoautotrophic



- chassis through systematic genome mapping and validation of neutral sites. *DNA Res.*, **22**, 425–437.
- Pye, C.R., Bertin, M.J., Lokey, R.S., Gerwick, W.H., Lington, R.G. (2017) Retrospective analysis of natural products provides insights for future discovery trends. *Proc. Natl. Acad. Sci. U.S.A.*, **114**, 5601–5606.
- Qi, Q., Hao, M., Ng, W., Slater, S.C., Baszis, S.R., Weiss, J.D., Valentin, H.E. (2005) Application of the *Synechococcus nirA* promoter to establish an inducible expression system for engineering the *Synechocystis* tocopherol pathway. *Appl. Environ. Microbiol.*, **71**, 5678–5684.
- Qi, L.S., Larson, M.H., Gilbert, L.A., Doudna, J.A., Weissman, J.S. Arkin, A.P., Lim, W.A. (2013) Repurposing CRISPR as an RNA-guided platform for sequence-specific control of gene expression. *Cell*, **152**, 1173–1183.
- Rae, B.D., Long, B., Förster, B., Nguyen, N.D., Velanis, C.N., Atkinson, N., Hee, W., Mukherjee, B., Price, G.D., McCormick, A.J. (2017) Progress and challenges of engineering a biophysical carbon dioxide concentrating mechanism into higher plants. *J. Ex. Bot.*, **68**, 3717–3737.
- Ramey, C.,J., Barón-Sola, Á., Aucoin, H.R., Boyle, N.R. (2015) Genome Engineering in Cyanobacteria: Where We Are and Where We Need To Go. *ACS Synth. Biol.*, **4**, 1186–1196.
- Rippka, R., Deruelles, J., Waterbury, J.B., Herdman, M., Stanier, R.Y. (1979) Generic assignments, strain histories and properties of pure cultures of cyanobacteria. *J. Gen. Microbiol.*, **111**, 1–61.
- Ruffing, A. M., Jensen, T. J., Strickland, L. M. (2016) Genetic tools for advancement of *Synechococcus* sp. PCC 7002 as a cyanobacterial chassis. *Microb. Cell Fact.*, **15**, 1–14.
- Saar, K.L., Bombelli, P., Lea-Smith, D.J., Call, T., Aro, E-M., Müller, T., Howe, C.J., Knowles, T.P.J. (2018) Enhancing power density of biophotovoltaics by decoupling storage and power delivery. *Nat. Energy*, **3**, 75–81.
- Sakai, Y., Abe, K., Nakashima, S., Ellinger, J.J., Ferri, S., Sode, K., Ikebukuro, K. (2015) Scaffold-fused riboregulators for enhanced gene activation in *Synechocystis* sp. PCC 6803. *MicrobiologyOpen*, **4**, 533–540.
- Sarrion-Perdigones, A., Vazquez-Vilar, M., Palací, J., Castelijns, B., Forment, J., Ziarsolo, P., Blanca, J., Granell, A., Orzaez, D. (2013) GoldenBraid 2.0: a comprehensive DNA assembly framework for plant synthetic biology. *Plant Physiol.*, **162**, 1618–1631.
- Shirai, T., Osanai, T. Kondo, A. (2016) Designing intracellular metabolism for production of target compounds by introducing a heterologous metabolic reaction based on a *Synechocystis* sp. 6803 genome-scale model. *Microb. Cell Fact.*, **15**, 13.
- Silva-Rocha, R., Martínez-García, E., Calles, B., Chavarría, M., Arce-Rodríguez, A., de Las Heras, A., Páez-Espino, A.D., Durante-Rodríguez, G., Kim, J., Nikel, P.I., Platero, R., de Lorenzo, V. (2013) The Standard European Vector Architecture (SEVA): a coherent platform for the analysis and deployment of complex prokaryotic phenotypes. *Nucleic Acids Res.* **41**, D666–675.
- Smanski, M.J., Zhou, H., Claesen, J., Shen, B., Fischbach, M.A., Voigt, C.A. (2016) Synthetic biology to access and expand nature's chemical diversity. *Nat. Rev. Microbiol.*, **14**, 135–149.
- Stensjö, K., Vavitsas, K., Tyystjärvi, T. (2017) Harnessing transcription for bioproduction in cyanobacteria. *Physiol. Plant*, **162**, 148–155.
- Stucken, K., Ilhan, J., Roettger, M., Dagan, T. Martin, W.F. (2012) Transformation and conjugal transfer of foreign genes into the filamentous multicellular cyanobacteria (subsection V) *Fischerella* and *Chlorogloeopsis*. *Curr. Microbiol.*, **65**, 552–560.

- Sun, T., Li, S., Song, X., Diao, J., Chen, L., Zhang, W. (2018) Toolboxes for cyanobacteria: Recent advances and future direction. *Biotechnol Adv.*, **36**, 1293–1307.
- Tan, X., Hou, S., Song, K., Georg, J., Klähn, S., Lu, X., Hess, W.R. (2017) The primary transcriptome of the fast-growing cyanobacterium *Synechococcus elongatus* UTEX 2973. *Biotechnol Biofuels.*, **11**, 218.
- Tan, X., Yao, L., Gao, Q., Wang, W., Qi, F., Lu, X. (2011) Photosynthesis driven conversion of carbon dioxide to fatty alcohols and hydrocarbons in cyanobacteria. *Metab. Eng.*, **13**, 169–176.
- Taton, A.,U., Ma, A.T., Ota, M., Golden, S.S., Golden, J.W. (2017) NOT gate genetic circuits to control gene expression in cyanobacteria. *ACS Synth. Biol.*, **6**, 2175–2182.
- Taton, A.,U., Unglaub, F. Wright, N.E., Zeng, W.Y., Paz-Yepes, J., Brahamsha, B., Palenik, B. Peterson, T.C., Haerizadeh, F., Golden, S.S., Golden, J.W. (2014) Broad-host-range vector system for synthetic biology and biotechnology in cyanobacteria. *Nucleic Acids Res.*, **42**, e136.
- Tsinoremas, N.F., Kutach, A.K., Strayer, C.A., Golden, S.S. (1994) Efficient gene transfer in *Synechococcus* sp. strains PCC 7942 and PCC 6301 by interspecies conjugation and chromosomal recombination. *J. Bacteriol.*, **176**, 6764–6768.
- Ungerer, J., Lin, P-C., Chen, H-Y., Pakrasi, H.B. (2018a) Adjustments to photosystem stoichiometry and electron transfer proteins are key to the remarkably fast growth of the cyanobacterium *Synechococcus elongatus* UTEX 2973. *mBio*, **9**, e02327–17.
- Ungerer, J., Pakrasi, H.B. (2016) Cpf1 Is a versatile tool for CRISPR genome editing across diverse species of cyanobacteria. *Sci. Rep.*, **6**, e39681.
- Ungerer, J., Wendt K.E., Hendry J.I., Marans C.D., Pakrasi, H.B. (2018b) Comparative genomics reveals the molecular determinants of rapid growth of the cyanobacterium *Synechococcus elongatus* UTEX 2973. *Proc. Natl. Acad. Sci. U.S.A.*, doi/10.1073/pnas.1814912115.
- van de Meene, A.M., Hohmann-Marriott, M.F., Vermaas, W.F., Roberson, R.W. (2006) The three-dimensional structure of the cyanobacterium *Synechocystis* sp. PCC 6803. *Arch Microbiol.*, **184**,259–270.
- Vazquez-Vilar M., Orzaez, D., Patron, N. (2018) DNA assembly standards: Setting the low-level programming code for plant biotechnology. *Plant Sci.*, **273**, 33–41.
- Vioque, A. (2007) Transformation of Cyanobacteria. In: León,R., Galván,A., Fernández,E. (eds) Transgenic Microalgae as Green Cell Factories. Advances in Experimental Medicine and Biology, vol 616. Springer, New York, pp 12–22.
- Vogel, A.I.M., Lale,R., Hohmann-Marriott, M.F. (2017) Streamlining recombination-mediated genetic engineering by validating three neutral integration sites in *Synechococcus* sp. PCC 7002. *J. Biol. Eng.*, **11**, 19.
- Wang, B., Eckert, C., Maness, P-C., Yu, J. (2018) A genetic toolbox for modulating the expression of heterologous genes in the cyanobacterium *Synechocystis* sp. PCC 6803. *ACS Synth. Biol.*, **19**, 276–286.
- Watanabe S., Noda A., Ohbayashi R., Uchioko K., Kurihara A., Nakatake S., Morioka S., Kanasaki Y., Chibazakura T., Yoshikawa H. (2018) ParA-like protein influences the distribution of multi-copy chromosomes in cyanobacterium *Synechococcus elongatus* PCC 7942. *Microbiology*, **164**, 45–56.
- Wendt, K.E., Ungerer, J., Cobb,R .E., Zhao, H., Pakrasi, H.B. (2016) CRISPR/Cas9 mediated targeted mutagenesis of the fast growing cyanobacterium *Synechococcus elongatus* UTEX 2973. *Microb. Cell. Fact.*, **15**, e115
- Werner, S., Engler, C., Weber, E., Gruetzner, R., Marillonnet, S. (2012) Fast track assembly of multigene constructs using Golden Gate cloning and the MoClo system. *Bioeng. Bugs.* **3**, 38–43.

- Włodarczyk, A., Gnanasekaran, T., Nielsen, A.Z., Zulu, N.N., Mellor, S.B., Luckner, M., Thøfner, J.F.B., Olsen, C.E., Mottawie, M.S., Burow, M., Pribil, M., Feussner, I., Møller, B.L., Jensen, P.E. (2016) Metabolic engineering of light-driven cytochrome P450 dependent pathways into *Synechocystis* sp. PCC 6803. *Metab. Eng.*, **33**, 1–11.
- Xiao, A., Cheng, Z., Kong, L., Zhu, Z., Lin, S., Gao, G., Zhang, B. (2014) CasOT: a genome-wide Cas9/gRNA off-target searching tool. *Bioinformatics*, **30**, 1180–1182.
- Xu, Y., Alvey, R.M., Byrne, P.O., Graham, J.E., Shen, G., Bryant, D. A. (2011) Expression of genes in cyanobacteria: adaptation of endogenous plasmids as platforms for high-level gene expression in *Synechococcus* sp. PCC 7002. *Methods Mol. Biol.*, **684**, 273–293.
- Yao, L., Cengic, I., Anfelt, J., Hudson, E.P. (2015) Multiple gene repression in cyanobacteria using CRISPRi. *ACS Synth. Biol.*, **5**, 207–212.
- Yu, J., Liberton, M., Cliften, P.F., Head, R.D., Jacobs, J.M., Smith, R.D., Koppelaar, D.W., Brand, J.J., Pakrasi, H.B. (2015) *Synechococcus elongatus* UTEX 2973, a fast growing cyanobacterial chassis for biosynthesis using light and CO<sub>2</sub>. *Sci. Rep.*, **5**, 8132.
- Zess, E.K., Begemann, M.B., Pflieger, B.F. (2016) Construction of new synthetic biology tools for the control of gene expression in the cyanobacterium *Synechococcus* sp. strain PCC 7002. *Biotechnol. Bioeng.*, **113**, 424–432.
- Zerulla, K., Ludt, K., Soppa J. (2016) The ploidy level of *Synechocystis* sp. PCC 6803 is highly variable and is influenced by growth phase and by chemical and physical external parameters. *Microbiology*, **162**, 730–739.
- Zhou, J., Zhang, H., Meng, H., Zhu, H., Bao, G., Zhang, Y., Li, Y., Ma, Y. (2014) Discovery of a super-strong promoter enables efficient production of heterologous proteins in cyanobacteria. *Sci. Rep.*, **4**, 4500.

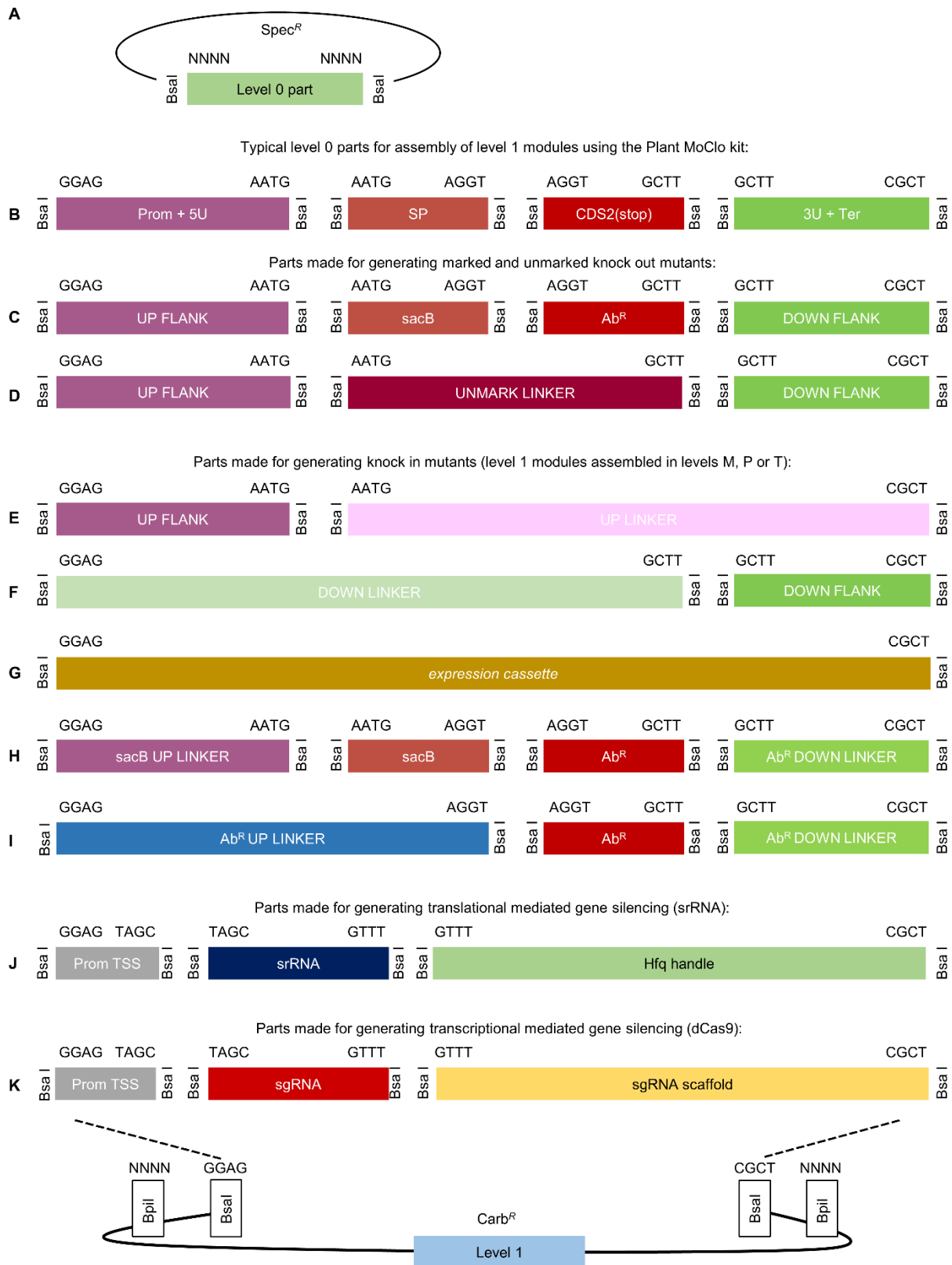


**Figure 1. Adaptation of the Plant Golden Gate MoClo level 0 syntax for generating level 1 assemblies for transfer to Level T.** (A) The format for a level 0 MoClo acceptor vector with the part bordered by two BsaI sites. (B) Typical level 0 parts from the Plant MoClo kit (38),

where parts of the same type are bordered by the same pair of fusion sites (for each fusion site, only the sequence of the top strand is shown). Note that the parts are not drawn to scale. (C, D) The syntax of the Plant MoClo kit was adapted to generate level 0 parts for engineering marked and unmarked cyanobacterial mutant strains (20). (E-I) To generate knock in mutants, short linker parts (30 bp) were constructed to allow assembly of individual flanking sequences, or marker cassettes ( $Ab^R$  or *sacB*) in level 1 vectors for subsequent assembly in level T. (J, K) Parts required for generating synthetic srRNA or CRISPRi level 1 constructs. See **Supplementary Information S3-S4** for workflows. Abbreviations: 3U+Ter, 3'UTR and terminator;  $Ab^R$ , antibiotic resistance cassette;  $Ab^R$  DOWN LINKER, short sequence (~30 bp) to provide CGCT overhang;  $Ab^R$  UP LINKER, short sequence (~30 bp) to provide GAGG overhang; CDS2(stop), coding sequence with a stop codon; DOWN FLANK, flanking sequence downstream of target site; DOWN FLANK LINKER, short sequence (~30 bp) to provide GGAG overhang; Prom+5U, promoter and 5' UTR; Prom TSS, promoter transcription start site; *sacB*, levansucrase expression cassette; *sacB* UP LINKER, short sequence (~30 bp) to provide GAGG overhang; sgRNA, single guide RNA; SP, signal peptide; srRNA, small regulatory RNA; UP FLANK, flanking sequence upstream of target site; UP FLANK LINKER, short sequence (~30 bp) to provide CGCT overhang; UNMARK LINKER, short sequence to bridge UP FLANK and DOWN FLANK.

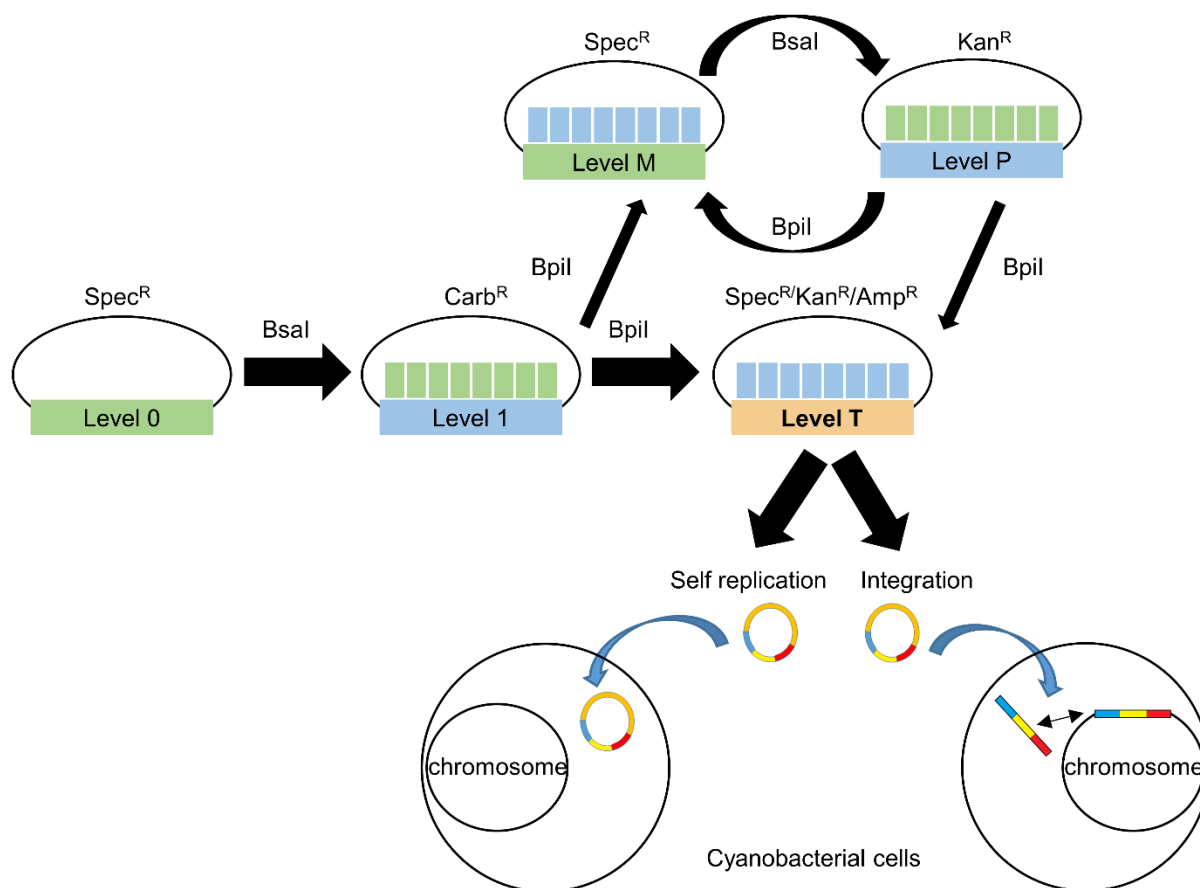


**Figure 2. Extension of the Plant Golden Gate MoClo Assembly Standard for cyanobacterial transformation.** Assembly relies on one of two Type IIS restriction endonuclease enzymes (*BsaI* or *BpiI*). Domesticated level 0 parts are assembled into level 1 vectors. Up to seven level 1 modules can be assembled directly into a level T cyanobacterial transformation vector, which consists of two sub-types (either a replicative or an integrative vector). Alternatively, larger vectors with more modules can be built by assembling level 1 modules into level M, and then cycling assembly between level M and level P, and finally transferred from Level P to level T. Antibiotic selection markers are shown for each level. Level T vectors are supplied with internal antibiotic selection markers (shown), but additional selection markers could be included from level 1 modules as required. **Supplementary Table S1** and **Supplementary Information S1**.

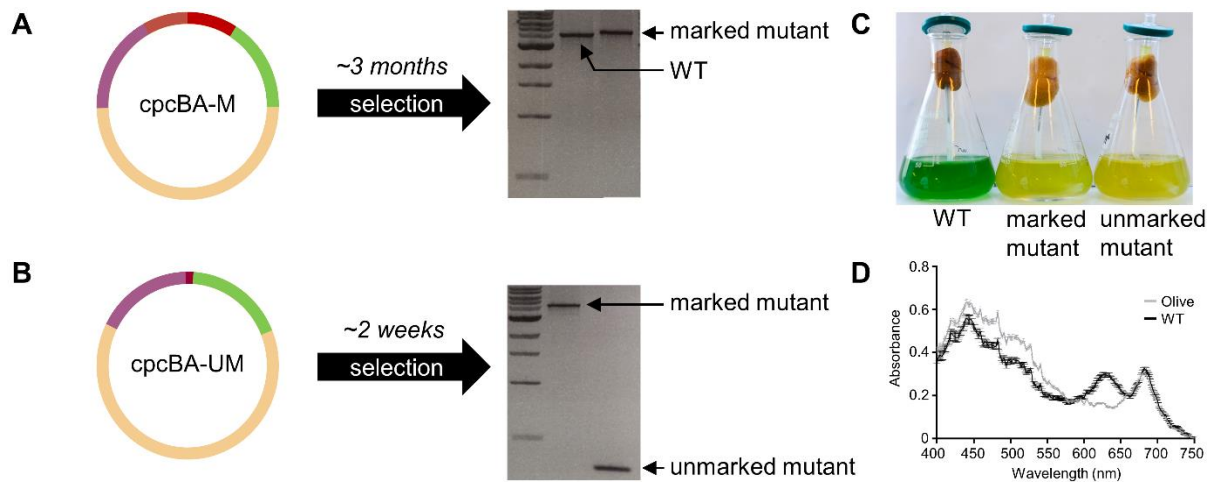


**Figure 3. Generating knock out mutants in cyanobacteria.** (A) Assembled level T vector *cpcBA-M* (see Fig. 1C) targeting the *cpcBA* promoter and operon (3,563 bp) to generate a marked  $\Delta cpcBA$  “Olive” mutant in *Synechocystis* sp. PCC 6803. Following transformation and segregation on Kanamycin (*ca.* 3 months), a segregated marked mutant was isolated (WT band is 3,925 bp, marked mutant band is 5,503 bp, 1kb DNA ladder (NEB) is shown). (B) Assembled level T vector *cpcBA-UM* (see Fig. 1D) for generating an unmarked  $\Delta cpcBA$  mutant. Following transformation and segregation on sucrose (*ca.* 2 weeks), an unmarked mutant was isolated (unmarked band is 425 bp). (C) Liquid cultures of WT, marked and unmarked Olive mutants. (D) Spectrum showing the absorbance of the unmarked Olive mutant and WT cultures after 72 hr of growth. Values are the average of four biological replicates  $\pm$  SE and are standardised to 750 nm.

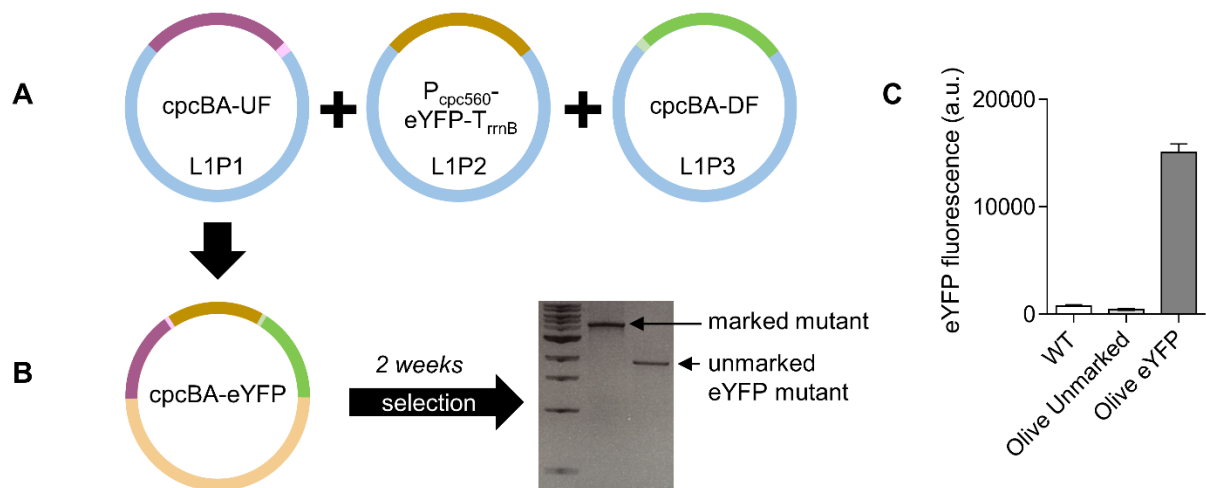


**Figure 4. Generating knock in mutants in cyanobacteria.** (A) Assembly of level 1 modules *cpcBA*-UF (see Fig. 1E) in the level 1, position 1 acceptor (L1P1),  $P_{cpc560}$ -eYFP-T<sub>rrmB</sub> (see Fig. 1G) in L1P2 and *cpcBA*-DF (see Fig. 1F) in L1P3. (B) Transfer of level 1 assemblies to level T vector *cpcBA*-eYFP for generating an unmarked  $\Delta cpcBA$  mutant carrying an eYFP expression cassette. Following transformation and segregation on sucrose (ca. 3 weeks), an unmarked eYFP mutant was isolated (1,771 bp). (C) Fluorescence values are the means  $\pm$  SE of four biological replicates, where each replicate represents the median measurements of 10,000 cells.



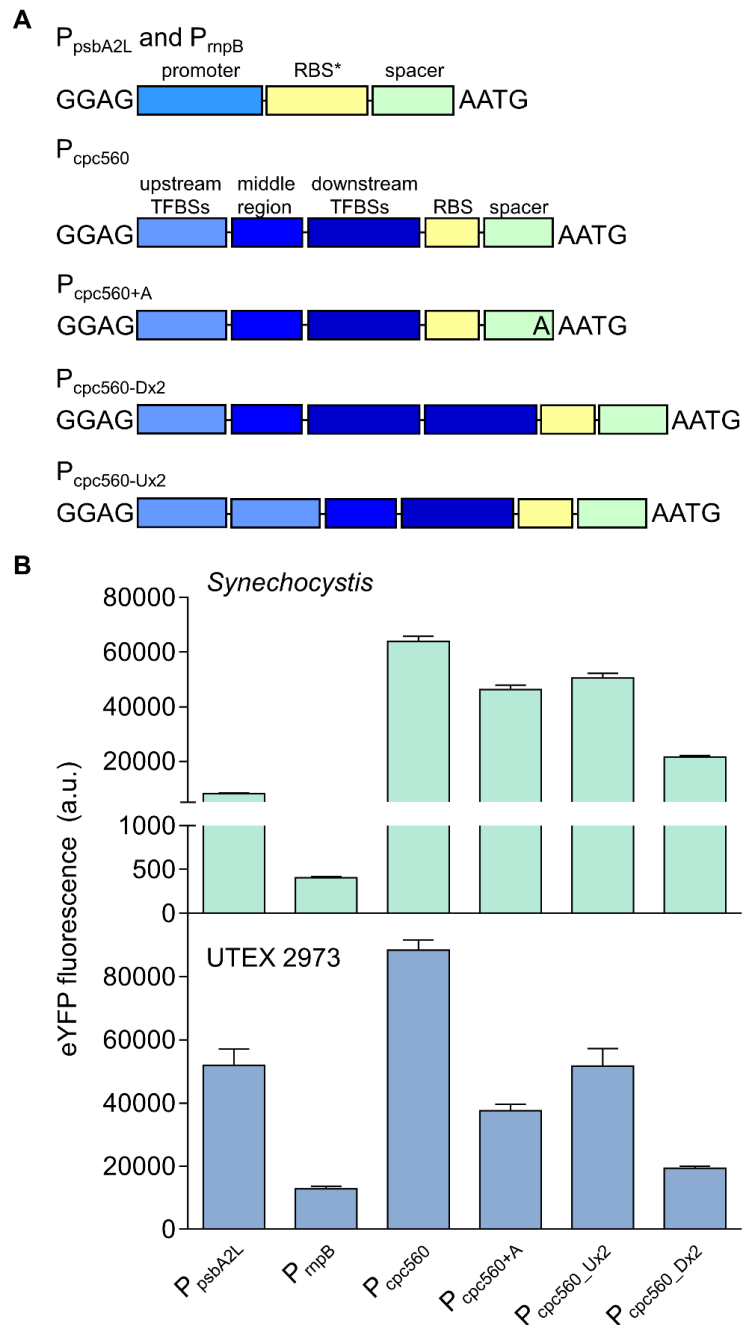


**Figure 5. Expression levels of cyanobacterial promoters in *Synechocystis* and UTEX 2973.**

(A) Structure of the cyanobacterial promoters adapted for the CyanoGate kit. Regions of  $P_{cpc560}$  shown are the upstream transcription factor binding sites (TFBSs) (-556 to -381 bp), middle region (-380 to -181 bp), and the downstream TFBSs, ribosome binding site (RBS) and spacer (-180 to -5 bp) (B) Expression levels of eYFP driven by promoters in *Synechocystis* and UTEX 2973 calculated from measurements taken from 10,000 individual cells. Values are the means  $\pm$  SE from at least four biological replicates after 48 hr of growth (average OD<sub>750</sub> values for *Synechocystis* and UTEX 2973 cultures were  $3.5 \pm 0.2$  and  $3.6 \pm 0.2$ , respectively). See **Supplementary Figure S2** for more info.

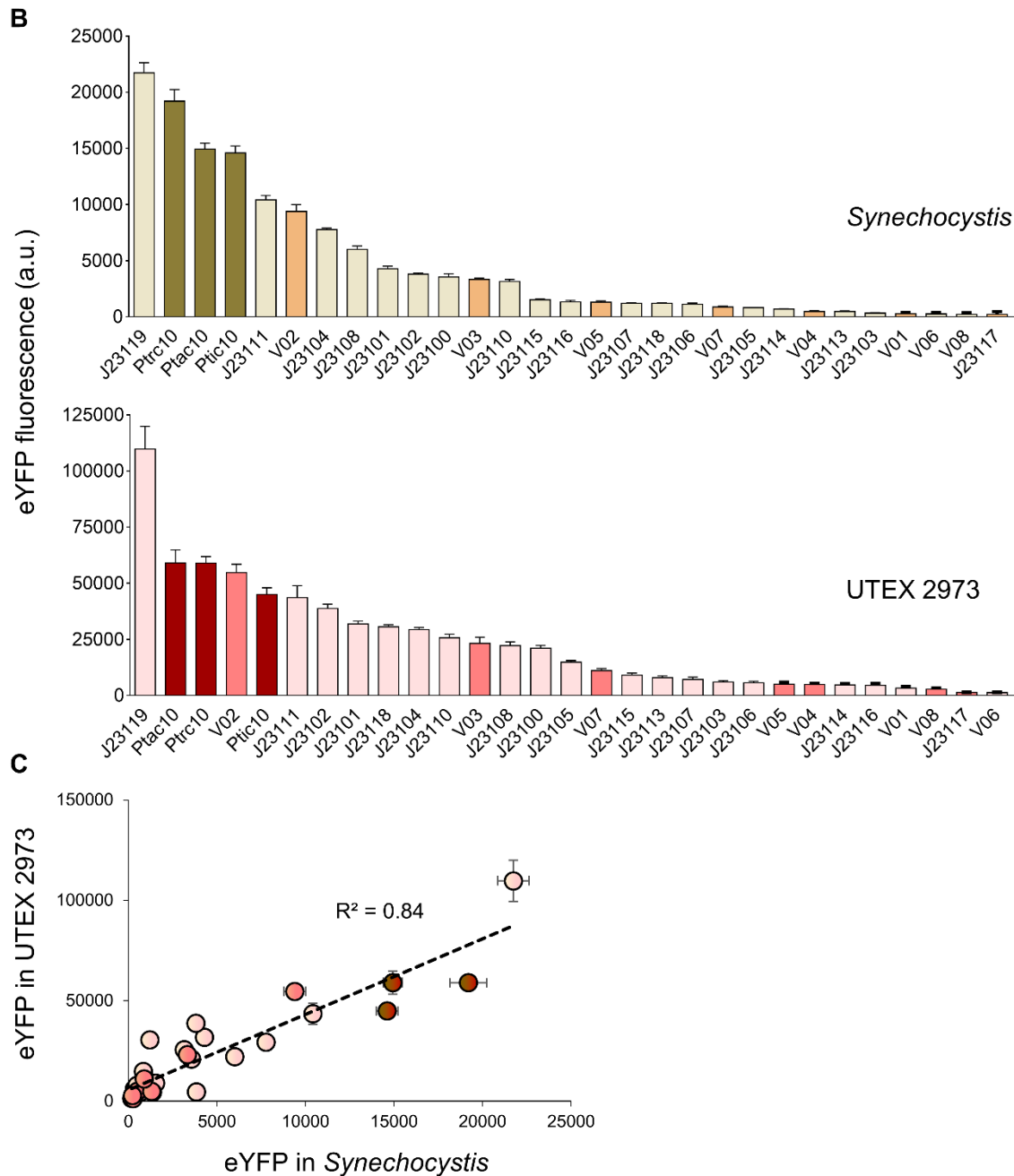
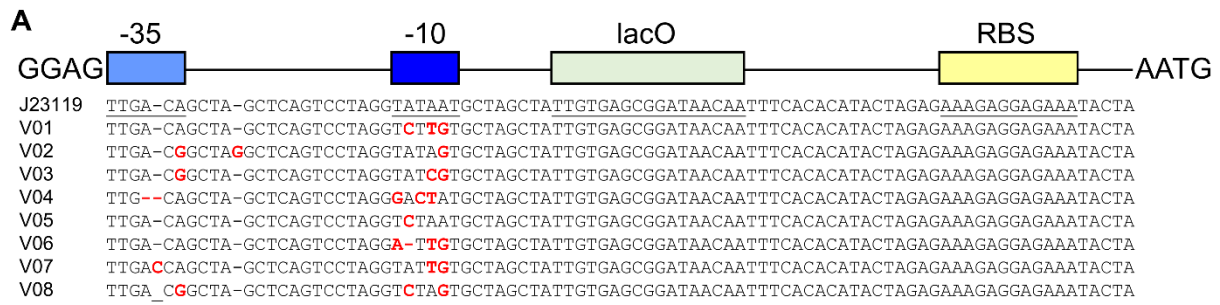


**Figure 6. Expression levels of heterologous and synthetic promoters in *Synechocystis* and UTEX 2973.** (A) Structure and alignment of eight new synthetic promoters derived from the BioBricks BBa\_J23119 library and  $P_{trc10}$  promoter design (18). (B) Expression levels of eYFP

driven by promoters in *Synechocystis* and UTEX 2973 calculated from measurements taken from 10,000 individual cells. (C) Correlation analysis of expression levels of synthetic promoters tested in *Synechocystis* and UTEX 2973. The coefficient of determination ( $R^2$ ) is shown for the J23119 library (red), new synthetic promoters (pink) and *trc* variants (dark red). Values are the means  $\pm$  SE from at least four biological replicates after 48 hr of growth (average  $OD_{750}$  values for *Synechocystis* and UTEX 2973 cultures were  $3.5 \pm 0.2$  and  $3.6 \pm 0.2$ , respectively). See **Supplementary Figure S2** for more info.

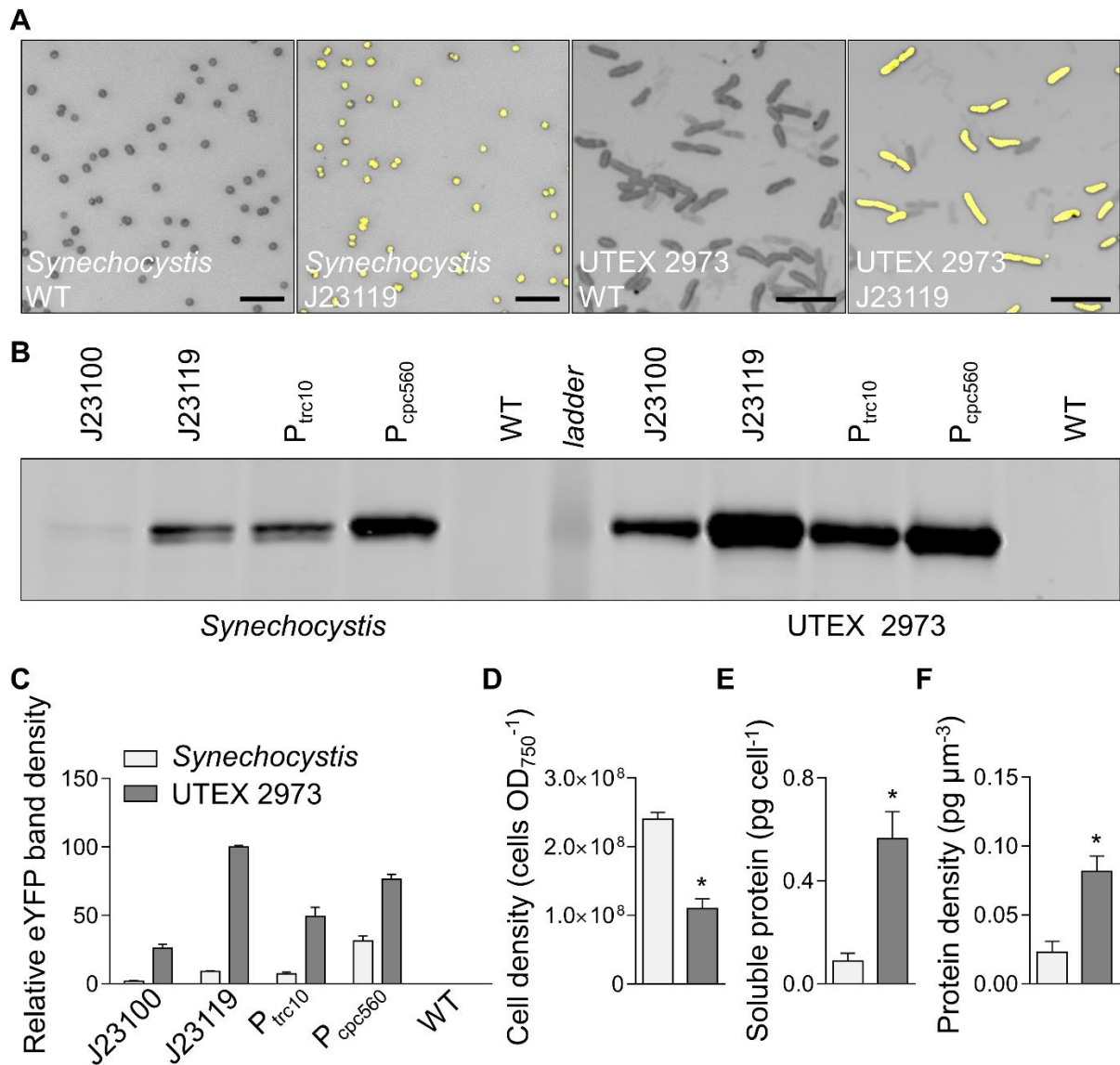


**Figure 7. Protein expression levels in *Synechocystis* and UTEX 2973 cells.** (A) Confocal images of WT strains and mutants expressing eYFP (fluorescence shown in yellow) driven by the J23119 promoter (bar = 10 μm). (B) Representative immunoblot of protein extracts (3 μg protein) from mutants with different promoter expression cassettes (as in Fig. 6) probed with an antibody against eYFP. The protein ladder band corresponds to 30 kDa. (C-E) Cell density, protein content per cell and protein density per estimated cell volume for *Synechocystis* and UTEX 2973. Asterisks (\*) indicate significant difference (P < 0.05) as determined by Student's *t*-tests. Values are the means ± SE of four biological replicates.

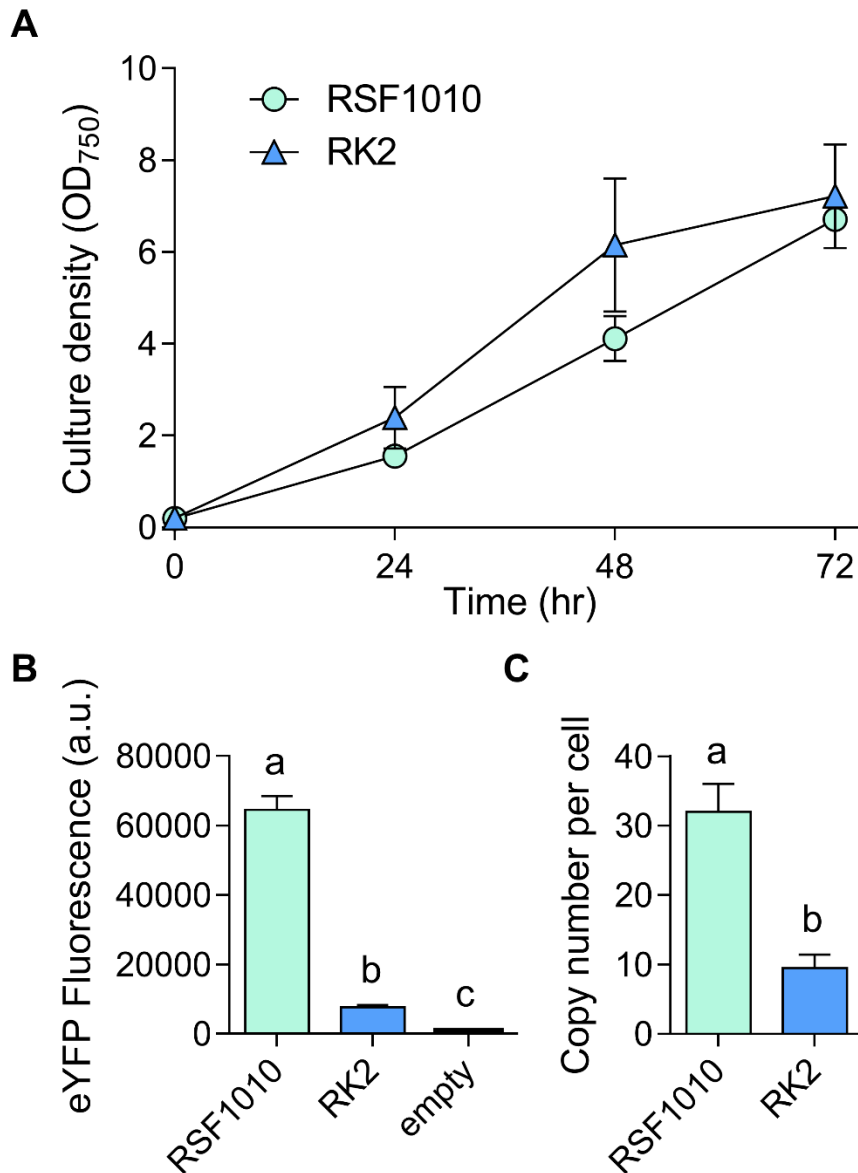


**Figure 8. Growth and expression levels of eYFP with the RK2 replicative origin in *Synechocystis*.** (A) Growth of strains carrying RK2 (vector pSEVA421-T-eYFP), RSF1010 (pPMQAK1-T-eYFP) or an empty pPMQAK1-T grown in appropriate antibiotics. Growth was measured as OD<sub>750</sub> under a constant illumination of 100  $\mu\text{mol photons m}^{-2}\text{s}^{-1}$  at 30 °C. (B) Expression levels of eYFP after 48 hr of growth calculated from measurements taken from 10,000 individual cells. (C) Plasmid copy numbers per cell after 48 hr of growth. Letters indicating significant difference ( $P < 0.05$ ) are shown, as determined by ANOVA followed by Tukey's HSD tests. Values are the means  $\pm$  SE of four biological replicates.

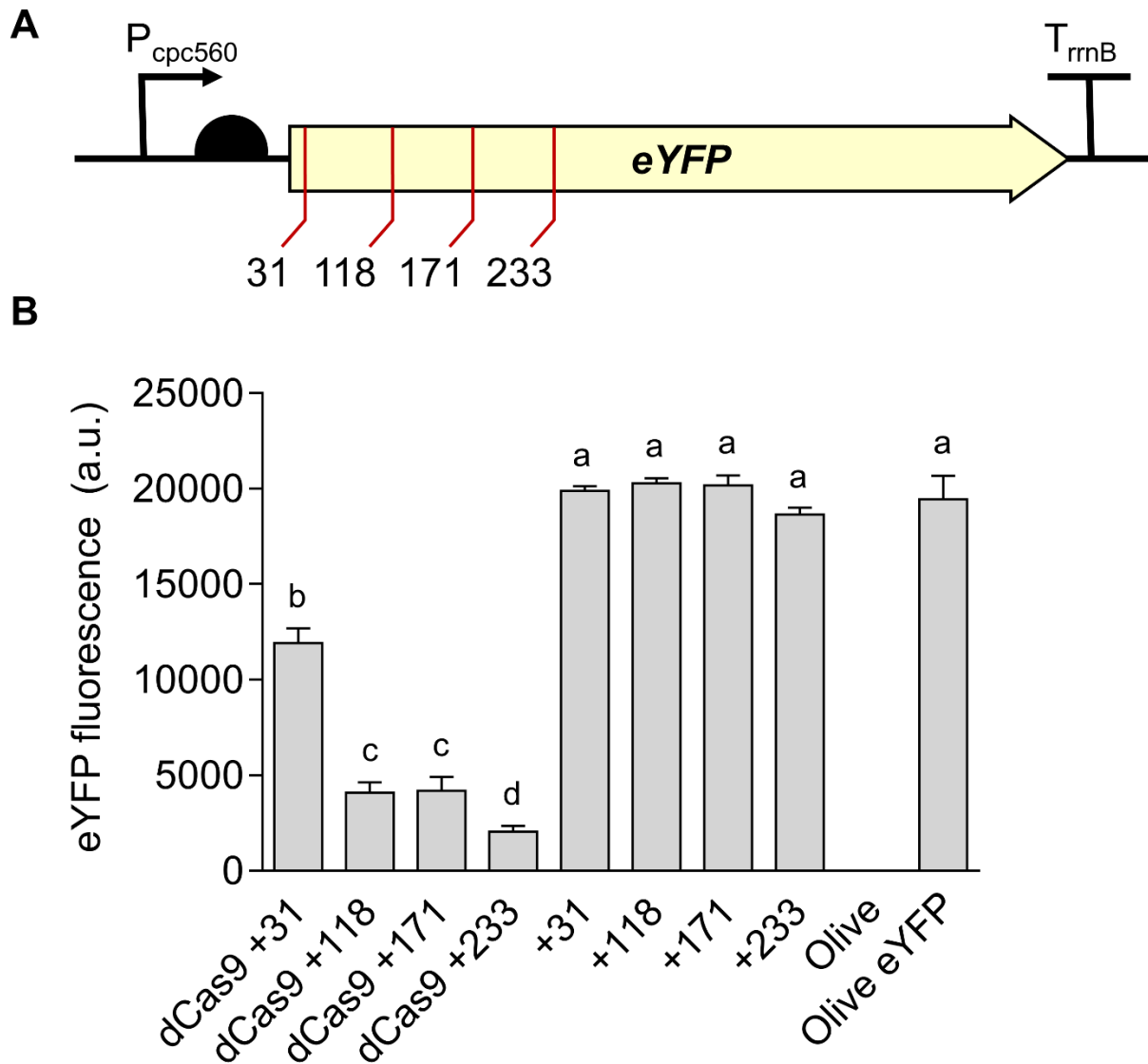


**Figure 9. Gene regulation system using CRISPRi in *Synechocystis*.** (A) Four target regions were chosen as sgRNA protospacers to repress eYFP expression in Olive-eYFP (**Fig. 4**): ‘CCAGGATGGGCACCACCC’ (+31), ‘ACTTCAGGGTCAGCTTGCCGT’ (+118), ‘AGGTGGTCACGAGGGTGGGCCA’ (+171) and ‘AGAAGTCGTGCTGCTTCATG’ (+233). (B) eYFP fluorescence of Olive-eYFP expressing constructs carrying sgRNAs with and without dCas9 (representative of 10,000 individual cells). Untransformed Olive-eYFP and the Olive mutant were used as controls. Letters indicating significant difference ( $P < 0.05$ ) are shown, as determined by ANOVA followed by Tukey’s HSD tests. Values are the means  $\pm$  SE of four biological replicates.

## SUPPLEMENTARY DATA

### **Supplementary Table S1. Table of all parts from CyanoGate kit generated in this work.**

Domestication refers to the removal of *BsaI* and/or *BsiI* sites (modifications are indicated in sequence maps provided in **Supp. Info. 2**). See separate .xlsx.

### **Supplementary Table S2. List of level T vectors used in this study.**

**Supplementary Table S3. Sequences of synthetic oligonucleotides used to determine copy number.** Primers used for amplifying the *petB* locus were from Pinto et al. (2012).

**Supplementary Information S1. Sequence maps (.gb files) of the components of the CyanoGate kit.** See .zip file.

**Supplementary Information S2. Protocols for MoClo assembly in level -1 through to level T.** Protocols for assembly in level 0, level M and level T acceptor vectors (restriction enzyme *BpiI* required, left). Protocols for assembly in level -1, level 1 and level P backbone vectors (restriction enzyme *BsaI* required, right). Adapted from “A quick guide to Type IIS cloning” (Patron Lab; [patronlab.org](http://patronlab.org)). For troubleshooting Type IIS mediated assembly we recommend [synbio.tsl.ac.uk/docs](http://synbio.tsl.ac.uk/docs).

**Supplementary Information S3. Detailed assembly strategies using the CyanoGate kit.**

**Supplementary Information S4. Integrative engineering strategies using the CyanoGate kit.** (A) Marked mutants are generated using a level T marked knock out vector carrying DNA sequences flanking the target locus of the chromosome (~1 kb), an antibiotic resistance cassette ( $Ab^R$ ) and a sucrose selection cassette (*sacB*) that produces the toxic compound levansucrase in the presence of sucrose (20). Several rounds of segregation are required to identify a marked mutant. (B) Marked mutants then can be unmarked with a level T unmarked knock out vector and selection on sucrose-containing agar plates. (C) Unmarked knock in mutants can also be generated from marked mutants using a level T unmarked knock in vector carrying a gene expression cassette (UP FLANK LINKER and DOWN FLANK LINKER are shown in pink and light green, respectively). (D) Alternatively marked knock in mutants can be engineered in a single step using a level T marked knock vector ( $Ab^R$  UP LINKER and DOWN LINKER are shown in blue and orange, respectively). See **Fig. 2** for abbreviations.

**Supplementary Information S5. Comparison of Gibson Assembly and Golden Gate Assembly.** (A) A comparison of Gibson Assembly and Golden Gate Assembly pathways for building the level T vector *cpcBA-eYFP* described in **Fig. 4**. (B) Advantages and disadvantages of Gibson Assembly and Golden Gate Assembly.

**Supplementary Information S6. Protocol and online interface for building CyanoGate vector assemblies.** A CyanoGate online vector assembly tool called Design and Build (DAB) from the Edinburgh Genome Foundry.

**Supplementary Figure S1. Comparison of growth for *Synechocystis*, PCC 7942 and UTEX 2973 under different culturing conditions.** Values are the means  $\pm$  SE from at least five biological replicates from two independent experiments.

**Supplementary Figure S2. Growth and expression levels of heterologous and synthetic promoters in *Synechocystis* and UTEX 2973.** (A) *Synechocystis* and UTEX 2973 was cultured for 72 hr at 30°C with continuous light ( $100 \mu\text{mol photons m}^{-2} \text{s}^{-1}$ ) and 40°C with  $300 \mu\text{mol photons m}^{-2} \text{s}^{-1}$ , respectively (see **Fig. 6**). Expression levels of eYFP are shown at three time points (24, 48 and 72 hr after inoculation). Values are the means  $\pm$  SE from at least four biological replicates where each replicate represents the median measurements of 10,000 cells

**Supplementary Figure S3. Cell volume calculations for *Synechocystis* and UTEX 2973 from confocal microscopy images.** (A) Example confocal images of *Synechocystis* (left) and UTEX 2973 (right) cells expressing eYFP driven by the J23119 promoter at 48 hr. Individual cells were selected and measured using Leica AF Lite software (Leica Microsystems). Top panel: eYFP fluorescence (green); middle panel: chlorophyll auto fluorescence (red); bottom panel: overlay of eYFP and chlorophyll signals (yellow). (B) Volume estimations based on confocal image data ( $n = 50$ ) (C) Mathematical formulas used for calculating cell volume based on the cell shapes of *Synechocystis* (coccus, spherical) and UTEX 2973 (bacillus, cylindrical).



Supplementary Table S2. List of level T vectors used in this study.

Vector ID	Part name	Acceptor backbone	Level 1 vectors	Selection	Notes
<b><u>Assembled Level T vector (integrative)</u></b>					
pCAT.336	pUC19A-T (cpcBA-M)		1		Generated a marked mutant in the cpcBA promoter and operon (Fig. 3). Generated an unmarked mutant in the cpcBA promoter and operon (Fig. 3). Introduced a eYFP expression cassette into the marked $\Delta$ cpcBA “Olive” mutant (Fig. 4).
pCAT.337	pUC19A-T (cpcBA-UM)	pUC19A-T	1	Amp <sup>R</sup>	
pCAT.312	pUC19A-T (cpcBA-eYFP)		3		
<b><u>Assembled Level T vector (replicative)</u></b>					
pCAT.9	pSEVA431-T	pSEVA431 Level T	-		Level T Acceptor, pBBR1 replicative origin (50). Level T Acceptor, pRO1600/ColE1 replicative origin (50). Level T assembly with eYFP expression cassette, RK2 replicative origin (Fig. 8) (50).
pCAT.13	pSEVA442-T	pSEVA442 Level T	-		
pCAT.163	pSEVA421-T (P <sub>cpc560</sub> -eYFP-T <sub>rrnB</sub> )	pSEVA421-T	1	Spec <sup>R</sup>	
pCAT.214	pPMQAK1-T (J23100 MH-eYFP-T <sub>rrnB</sub> )		1		Level T assemblies with eYFP expression cassette (Fig. 5-7) (18), pPMQAK1-T replicative origin.
pCAT.235	pPMQAK1-T (J23101MH-eYFP-T <sub>rrnB</sub> )		1		
pCAT.236	pPMQAK1-T (J23102MH-eYFP-T <sub>rrnB</sub> )		1		
pCAT.237	pPMQAK1-T (J23103MH-eYFP-T <sub>rrnB</sub> )		1		
pCAT.238	pPMQAK1-T (J23104MH-eYFP-T <sub>rrnB</sub> )	pPMQAK1-T	1	Amp <sup>R</sup> , Kan <sup>R</sup>	
pCAT.239	pPMQAK1-T (J23105MH-eYFP-T <sub>rrnB</sub> )		1		
pCAT.240	pPMQAK1-T (J23106MH-eYFP-T <sub>rrnB</sub> )		1		
pCAT.241	pPMQAK1-T (J23107MH-eYFP-T <sub>rrnB</sub> )		1		

## A Golden Gate-based toolkit for engineering cyanobacteria

pCAT.242	pPMQAK1-T (J23108MH-eYFP- T <sub>rrnB</sub> )	1
pCAT.243	pPMQAK1-T (J23109MH-eYFP- T <sub>rrnB</sub> )	1
pCAT.244	pPMQAK1-T (J23110MH-eYFP- T <sub>rrnB</sub> )	1
pCAT.245	pPMQAK1-T (J23111MH-eYFP- T <sub>rrnB</sub> )	1
pCAT.193	pPMQAK1-T (J23113MH-eYFP- T <sub>rrnB</sub> )	1
pCAT.247	pPMQAK1-T (J23114MH-eYFP- T <sub>rrnB</sub> )	1
pCAT.248	pPMQAK1-T (J23115MH-eYFP- T <sub>rrnB</sub> )	1
pCAT.249	pPMQAK1-T (J23116MH-eYFP- T <sub>rrnB</sub> )	1
pCAT.250	pPMQAK1-T (J23117MH-eYFP- T <sub>rrnB</sub> )	1
pCAT.251	pPMQAK1-T (J23118MH-eYFP- T <sub>rrnB</sub> )	1
pCAT.252	pPMQAK1-T (BBa_J23119MH- eYFP-T <sub>rrnB</sub> )	1
pCAT.253	pPMQAK1-T (P <sub>psbA2L</sub> -eYFP-T <sub>rrnB</sub> )	1
pCAT.254	pPMQAK1-T (P <sub>mpB</sub> - eYFP-T <sub>rrnB</sub> )	1
pCAT.262	pPMQAK1-T (P <sub>trc10</sub> - eYFP-T <sub>rrnB</sub> )	1
pCAT.263	pPMQAK1-T (P <sub>tac10</sub> - eYFP-T <sub>rrnB</sub> )	1
pCAT.264	pPMQAK1-T (P <sub>tic10</sub> - eYFP-T <sub>rrnB</sub> )	1
pCAT.267	pPMQAK1-T (J23119MH_V01- eYFP-T <sub>rrnB</sub> )	1
pCAT.268	pPMQAK1-T (J23119MH_V02- eYFP-T <sub>rrnB</sub> )	1
pCAT.269	pPMQAK1-T (J23119MH_V03- eYFP-T <sub>rrnB</sub> )	1
pCAT.272	pPMQAK1-T (J23119MH_V04- eYFP-T <sub>rrnB</sub> )	1
pCAT.273	pPMQAK1-T (J23119MH_V05- eYFP-T <sub>rrnB</sub> )	1

## A Golden Gate-based toolkit for engineering cyanobacteria

pCAT.274	pPMQAK1-T (J23119MH_V06- eYFP-T <sub>rrnB</sub> )	1			
pCAT.265	pPMQAK1-T (J23119MH_V07- eYFP-T <sub>rrnB</sub> )	1			
pCAT.266	pPMQAK1-T (J23119MH_V08- eYFP-T <sub>rrnB</sub> )	1			
pCAT.278	pPMQAK1-T (P <sub>cpc560</sub> +A-eYFP- T <sub>rrnB</sub> )	1			
pCAT.279	pPMQAK1-T (P <sub>cpc560</sub> -eYFP-T <sub>rrnB</sub> )	1			
pCAT.280	pPMQAK1-T (P <sub>cpc560</sub> - Ux2-eYFP-T <sub>rrnB</sub> )	1			
pCAT.281	pPMQAK1-T (P <sub>cpc560</sub> - Dx2-eYFP-T <sub>rrnB</sub> )	1			
pCAT.314	pPMQAK1-T (P <sub>cpc560</sub> -dCas9-T <sub>rrnB</sub> ) + (P <sub>trc10_TSS</sub> - sgRNA+31-sgRNA scaffold)	2			
pCAT.315	pPMQAK1-T (P <sub>cpc560</sub> -dCas9-T <sub>rrnB</sub> ) + (P <sub>trc10_TSS</sub> - sgRNA+118-sgRNA scaffold)	2			
pCAT.316	pPMQAK1-T (P <sub>cpc560</sub> -dCas9-T <sub>rrnB</sub> ) + (P <sub>trc10_TSS</sub> - sgRNA+171-sgRNA scaffold)	2			
pCAT.317	pPMQAK1-T (P <sub>cpc560</sub> -dCas9-T <sub>rrnB</sub> ) + (P <sub>trc10_TSS</sub> - sgRNA+233-sgRNA scaffold)	2	pPMQAK1- T	AmpR, KanR	Level T assemblies for CRISPRi (Fig. 9) (81), pPMQAK1-T replicative origin.
pCAT.319	pPMQAK1-T (P <sub>trc10_TSS</sub> - sgRNA+31-sgRNA scaffold)	1			
pCAT.320	pPMQAK1-T (P <sub>trc10_TSS</sub> - sgRNA+118-sgRNA scaffold)	1			
pCAT.321	pPMQAK1-T (P <sub>trc10_TSS</sub> - sgRNA+171-sgRNA scaffold)	1			
pCAT.322	pPMQAK1-T (P <sub>trc10_TSS</sub> - sgRNA+233-sgRNA scaffold)	1			

**Supplementary Table S3. Sequences of synthetic oligonucleotides used to determine copy number.** Primers used for amplifying the *petB* locus were from Pinto et al. (2012).

Name	Locus	Amplicon length (bp)	Forward primer	Reverse primer
pPMQAK1-T (RSF1010)	-	245	AGTTAAGCCAGCCCCGACAC C	TTGAGTGAGCTGATACCGCT
pSEVA421-T (RK2)	-	135	ACGACCAAGAAGCGAAAAAC C	CCACGGCGCAATATCGAAC
<i>petB</i> locus	-	1000	ATAGTACGCTGATTATATGCG ATTTTACGG	CATGTAAAGAATGTCGTTGGG CCA
<i>petB</i>	slr0342 (Chr:2647386-2650184)	179	CCTTCGCCTCTGTCCAATAC	TAGCATTACACCCACAACCC
<i>secA</i> locus	-	1000	CATAACCTTCTTGCTTATATTC AATCAAGGGA	AGCCAGGAAACGGAAGACTT AC
<i>secA</i>	slr0616 (Chr:2428010-2428678)	113	TAAATCCAAACCTTCCAGCA CCC	AACCTATTACTACGACATCCG TAAGC

**Supplementary Information S2. Protocols for MoClo assembly in level -1 through to level T.** Protocols for assembly in level 0, level M and level T acceptor vectors (restriction enzyme *BpiI* required, left). Protocols for assembly in level -1, level 1 and level P backbone vectors (restriction enzyme *BsaI* required, right). Adapted from “A quick guide to Type IIS cloning” (Patron Lab; [patronlab.org](http://patronlab.org)). For troubleshooting Type IIS mediated assembly we recommend [synbio.tsl.ac.uk/docs](http://synbio.tsl.ac.uk/docs).

***BpiI* protocol (in restriction buffer)**

- 50-100 ng of acceptor vector.
- For each modular vector/part to insert, use a 2:1 ratio of insert: acceptor.
- 2  $\mu$ l 10 mM ATP (not dATP).
- 2  $\mu$ l Buffer G (ThermoFisher).
- 2  $\mu$ l BSA (10X).
- 10 units *BpiI*  
(1  $\mu$ l 10 U/ $\mu$ l *BpiI*, ThermoFisher)
- 200 units T4 DNA ligase  
(1  $\mu$ l 200U/ $\mu$ l, ThermoFisher)

37<sup>o</sup> C for 10 minutes  
16<sup>o</sup> C for 10 minutes  
37<sup>o</sup> C for 20 minutes  
65<sup>o</sup> C for 10 minutes  
16<sup>o</sup> C (hold)

| X5

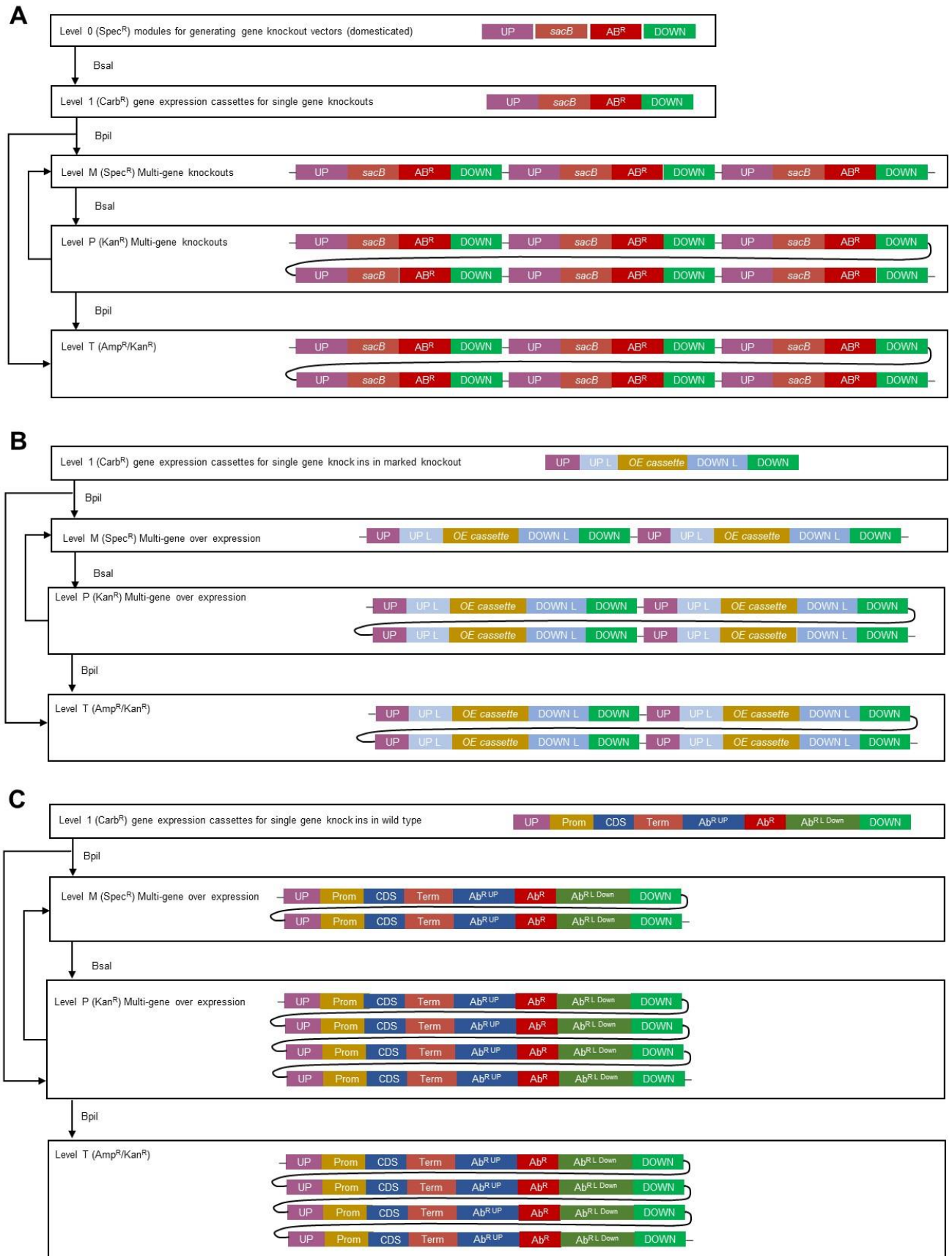
***BsaI* protocol (in restriction buffer)**

- 50-100 ng of acceptor vector.
- For each modular vector/part to insert, use a 2:1 ratio of insert: acceptor.
- 2  $\mu$ l 10 mM ATP (not dATP).
- 2  $\mu$ l Buffer G (ThermoFisher).
- 2  $\mu$ l BSA (10X).
- 10 units *BsaI*  
(1  $\mu$ l 10 U/ $\mu$ l *BsaI*, ThermoFisher)
- 200 units T4 DNA ligase  
(1  $\mu$ l 200U/ $\mu$ l, ThermoFisher)

37<sup>o</sup> C for 10 minutes  
16<sup>o</sup> C for 10 minutes  
37<sup>o</sup> C for 20 minutes  
65<sup>o</sup> C for 10 minutes  
16<sup>o</sup> C (hold)

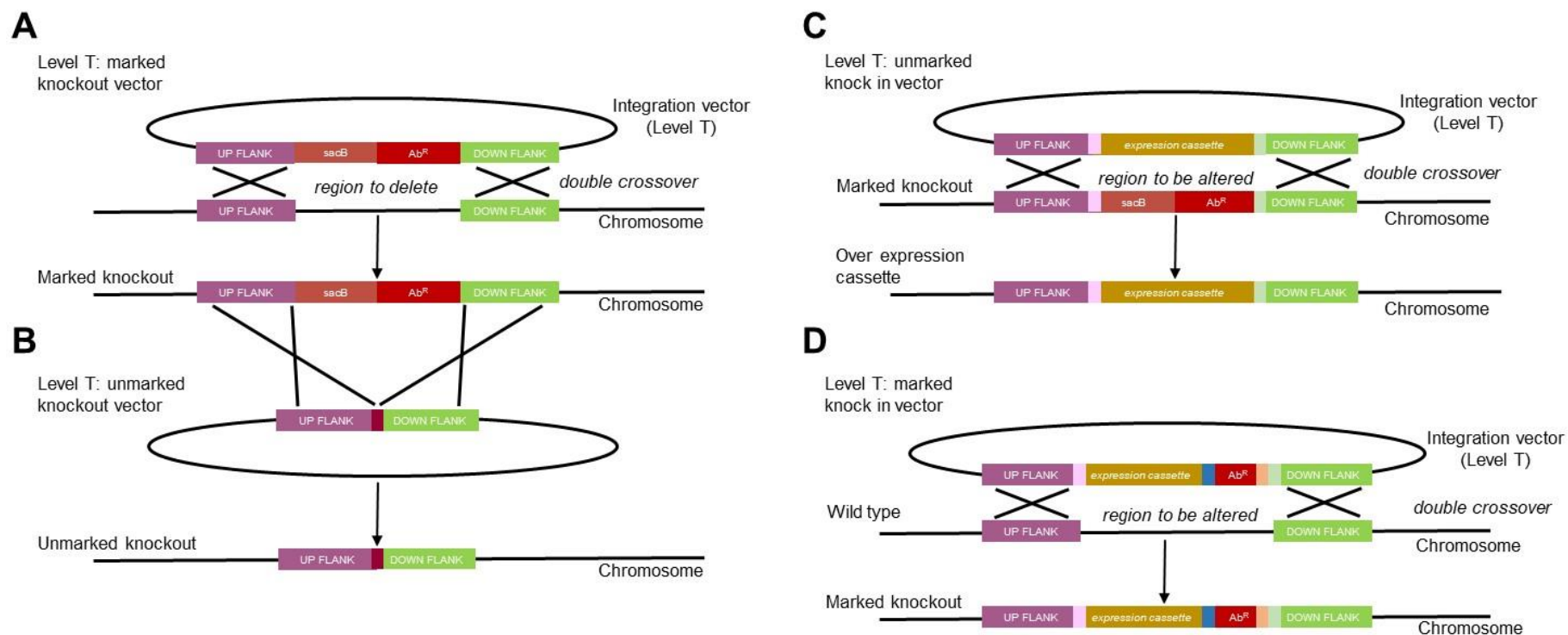
| X5

Supplementary Information S3. Detailed assembly strategies using the CyanoGate kit.

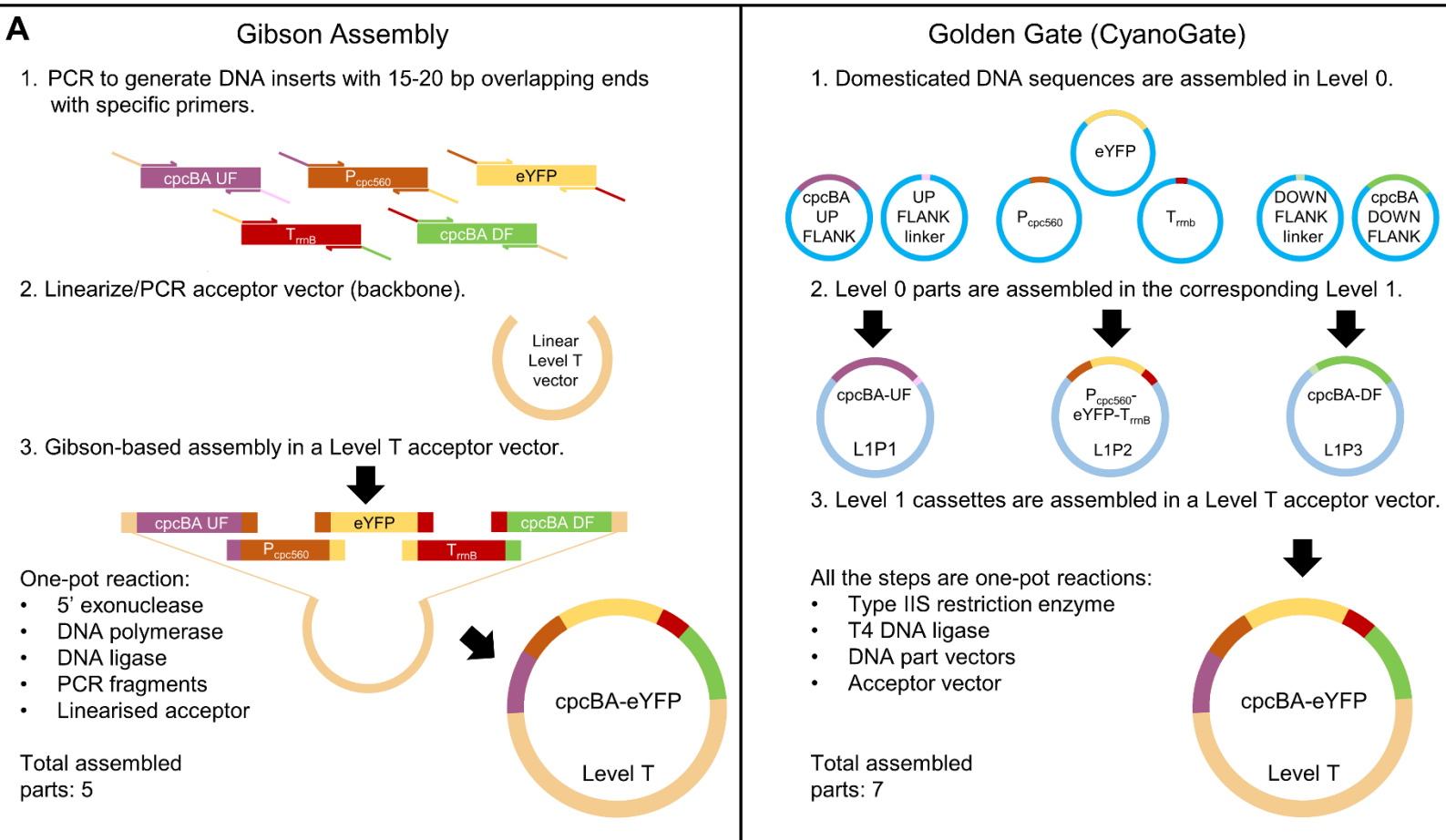


## A Golden Gate-based toolkit for engineering cyanobacteria

**Supplementary Information S4. Integrative engineering strategies using the CyanoGate kit.** (A) Marked mutants are generated using a level T marked knock out vector carrying DNA sequences flanking the target locus of the chromosome (~1 kb), an antibiotic resistance cassette ( $Ab^R$ ) and a sucrose selection cassette (*sacB*) that produces the toxic compound levansucrase in the presence of sucrose (20). Several rounds of segregation are required to identify a marked mutant. (B) Marked mutants then can be unmarked with a level T unmarked knock out vector and selection on sucrose-containing agar plates. (C) Unmarked knock in mutants can also be generated from marked mutants using a level T unmarked knock in vector carrying a gene expression cassette (UP FLANK LINKER and DOWN FLANK LINKER are shown in pink and light green, respectively). (D) Alternatively marked knock in mutants can be engineered in a single step using a level T marked knock vector ( $Ab^R$  UP LINKER and DOWN LINKER are shown in blue and orange, respectively). See **Fig. 2** for abbreviations.



**Supplementary Information S5. Comparison of Gibson Assembly and Golden Gate Assembly.** (A) A comparison of Gibson Assembly and Golden Gate Assembly pathways for building the level T vector cpcBA-eYFP described in Fig. 4. (B) Advantages and disadvantages of Gibson Assembly and Golden Gate Assembly.



**B**

<b>Description</b>	<p><b>The Gibson Assembly (GA)</b> approach allows for the joining of two or more DNA fragments to generate plasmid vectors in a single isothermal reaction (Gibson et al., 2009).</p>	<p><b>The Golden Gate (GG) Assembly</b> approaches (e.g. MoClo and GoldenBraid) use Type IIS restriction enzymes (REs) to generate standardised, non-palindromic overhangs that enable ordered assembly of multiple DNA parts in a single digestion-ligation reaction (Vazquez-Vilar et al., 2018).</p>
<b>Advantages</b>	<ul style="list-style-type: none"> <li>• Virtually any DNA fragments and any plasmid can be assembled together without prior modifications.</li> <li>• Allows seamless (scarless), directional cloning of multiple DNA fragments.</li> <li>• Can be used for cloning a wide range of DNA fragment sizes (i.e. 100-100,000 bp).</li> </ul>	<ul style="list-style-type: none"> <li>• Can re-use parts without modification in new assemblies.</li> <li>• Once parts are made, no subsequent PCR or clean-ups steps are required, and new assemblies do not require sequence checking.</li> <li>• GG only requires liquid handling (no columns or gels) so can be automated. Thus, GG is simple to scale for high-throughput protocols (e.g. assembly of combinatorial libraries).</li> </ul>



## A Golden Gate-based toolkit for engineering cyanobacteria

<p><b>Advantages</b></p>	<ul style="list-style-type: none"> <li>• Depending on the number of fragments, GA can help to avoid multiple rounds of cloning (i.e. into different levels).</li> <li>• GA does not require DNA domestication (i.e. removal of incompatible restriction enzyme recognition sites).</li> <li>• Apart from vector assembly, GA can be used for numerous additional applications such, site-directed mutagenesis, library construction, shotgun cloning and the development of bacterial artificial chromosomes (BACs) (Li et al. 2018).</li> </ul>	<ul style="list-style-type: none"> <li>• GG allows for the standardisation of parts and vectors:-             <ul style="list-style-type: none"> <li>○ Standard overhangs allow for directional and hierarchical assembly.</li> <li>○ Assemblies are carried out with a common set of established acceptor vectors and a defined assembly protocol.</li> <li>○ Standard antibiotic selection markers and visual colony screening (e.g. blue/white) at each assembly level to facilitate the detection of positive colonies.</li> <li>○ Establishment of a common genetic syntax (i.e. the Phytobricks standard) has enabled broader exchange of parts and assemblies (Patron et al., 2015).</li> <li>○ GG simplifies experimental replication, and comparable information is available for part performance and methods for reliable assembly.</li> <li>○ The availability of libraries of standard exchangeable DNA parts (e.g. Phytobricks, MoClo).</li> </ul> </li> </ul>
<p><b>Disadvantages</b></p>	<ul style="list-style-type: none"> <li>• Primers for each part are needed for every assembly.</li> <li>• Unique overlapping primer pairs are required to join two different DNA fragments. This can limit the ability to freely combine different parts (e.g. for promoter screening).</li> <li>• PCR can fail.</li> <li>• Secondary structures and/or repetitive sequences in the overlap region can limit the efficiency and accuracy of assembly.</li> <li>• Sequence verification of all regions that undergo PCR amplification is recommended. Some DNA regions are challenging to sequence (e.g. the pPMQAK1 backbone), which can increase the cost of sequencing.</li> <li>• Assembly efficiencies decline with six or more DNA fragments or with the use of fragments shorter than 100 bp.</li> <li>• • Very small parts have to be first assembled by extension/overlap PCR.</li> </ul>	<ul style="list-style-type: none"> <li>• DNA parts and acceptor vectors require domestication to remove illegal Type IIS RE sites.</li> <li>• Some DNA sequences (e.g. promoters) may be challenging to domesticate due to the presence of RE sites in regulatory elements.</li> <li>• Assembly is quasi-seamless due to the use of standardised overhangs.</li> <li>• Initial setup can be time consuming, and purchase of Addgene kits could be a relatively costly starting investment.</li> </ul>

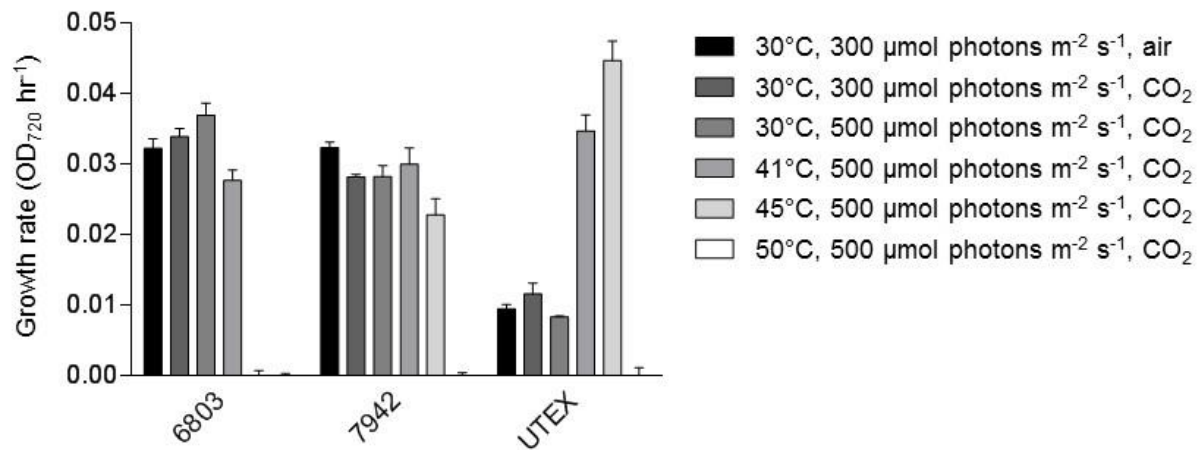
**Supplementary Information S6. Protocol and online interface for building CyanoGate vector assemblies.** A CyanoGate online vector assembly tool called Design and Build (DAB) from the Edinburgh Genome Foundry.

1. Site: [dab.genomefoundry.org](http://dab.genomefoundry.org)
2. Select “Home” and “Design New Assemblies”.
3. Select “MoClo”, then from the drop down list select “CyanoGate”.
4. There are 3 options: a) L1-knockout, b) L1-knock in, and c) L1-standard.
  - a. L1-knockout
    - This is a level 1 assembly for generating a marked or unmarked knockout mutant (see **Fig. 2**). The level 1 module(s) then should be transferred to the integrative level T integrative vector (pCAT15.UC19) for chromosomal integration in species amenable to natural transformation (e.g. *Synechocystis* sp. PCC 6803) (20).
    - Example of level 1 assembly for generating a level T knockout vector: L1P1 acceptor (DOWN FLANK + *sacB* + Ab<sup>R</sup>Kan + UP FLANK).
  - b. L1-knock in
    - This is a level 1 assembly for generating a knock in mutant (see **Fig. 3**). Each level 0 flanking region should be assembled into a specific level 1 position with gene expression cassettes (L1-standard) in between them.
    - The level 1 modules then should be transferred to the integrative level T integrative vector (pCAT15.UC19) for chromosomal integration in species amenable to natural transformation (e.g. *Synechocystis* sp. PCC 6803).
    - Example of 3 level 1 assemblies for generating a level T knock in vector: L1P1 acceptor (6803 NS1 Down Flank (slr0573) + DOWN FLANK), L1P2 acceptor (P<sub>trc10</sub> + eYFP + T<sub>rmB</sub>), L1P3 acceptor (UP FLANK + 6803 NS1 Up Flank (slr0573)).
  - c. L1-standard.
    - This is a level 1 assembly for generating a standard gene expression cassette from level 0 parts.
    - These level 1 modules can be transferred to the integrative level T integrative vector (pCAT15.UC19) for chromosomal integration in species amenable to natural transformation (e.g. *Synechocystis* sp. PCC 6803).
    - Alternatively, the level 1 modules can be transferred to a replicative level T vector (e.g. pCAT0.PMQAK1) for transformation into cyanobacterial species amenable to conjugation or electroporation.
    - Example of a level 1 assembly for generating a level T expression vector: L1P1 acceptor (P<sub>trc10</sub> + eYFP + T<sub>rmB</sub>).

**Figure 1.** Screenshot of the online “Design and Build” (DAB) tool ([dab.genomefoundry.org](http://dab.genomefoundry.org)) that allows users to browse parts and create structurally valid vector assemblies (1), choose from pre-defined templates (2), and order *in silico* assemblies directly from the foundry (3).

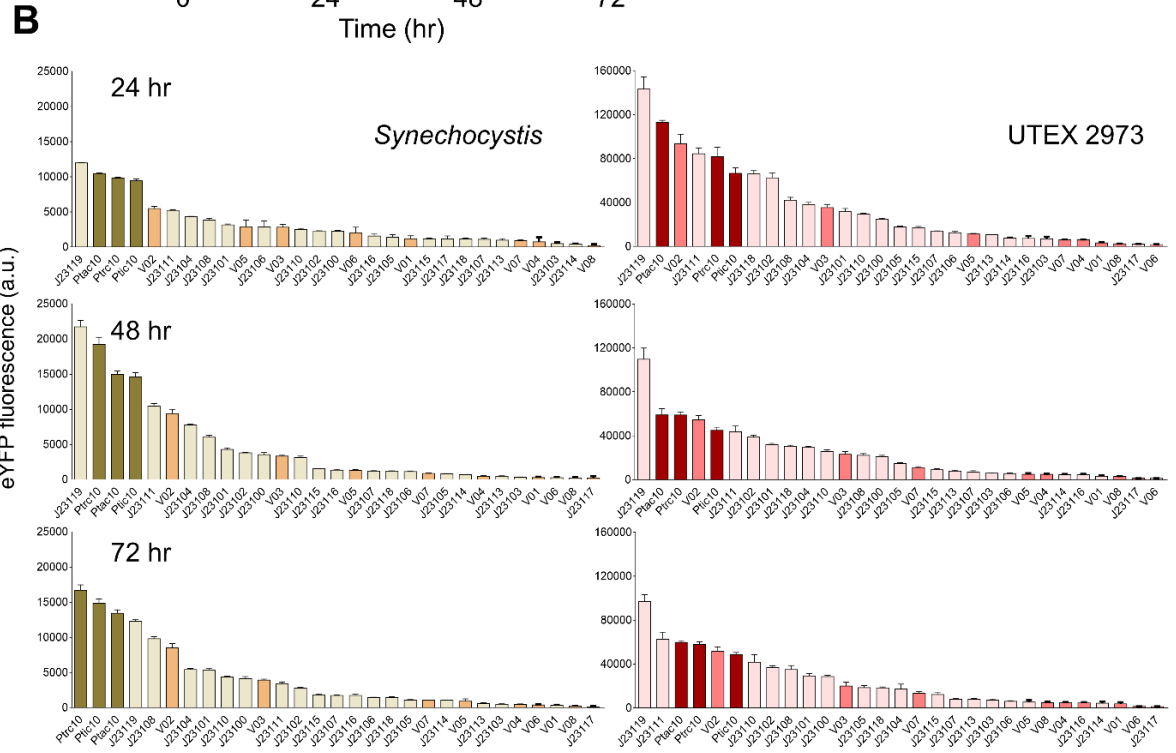
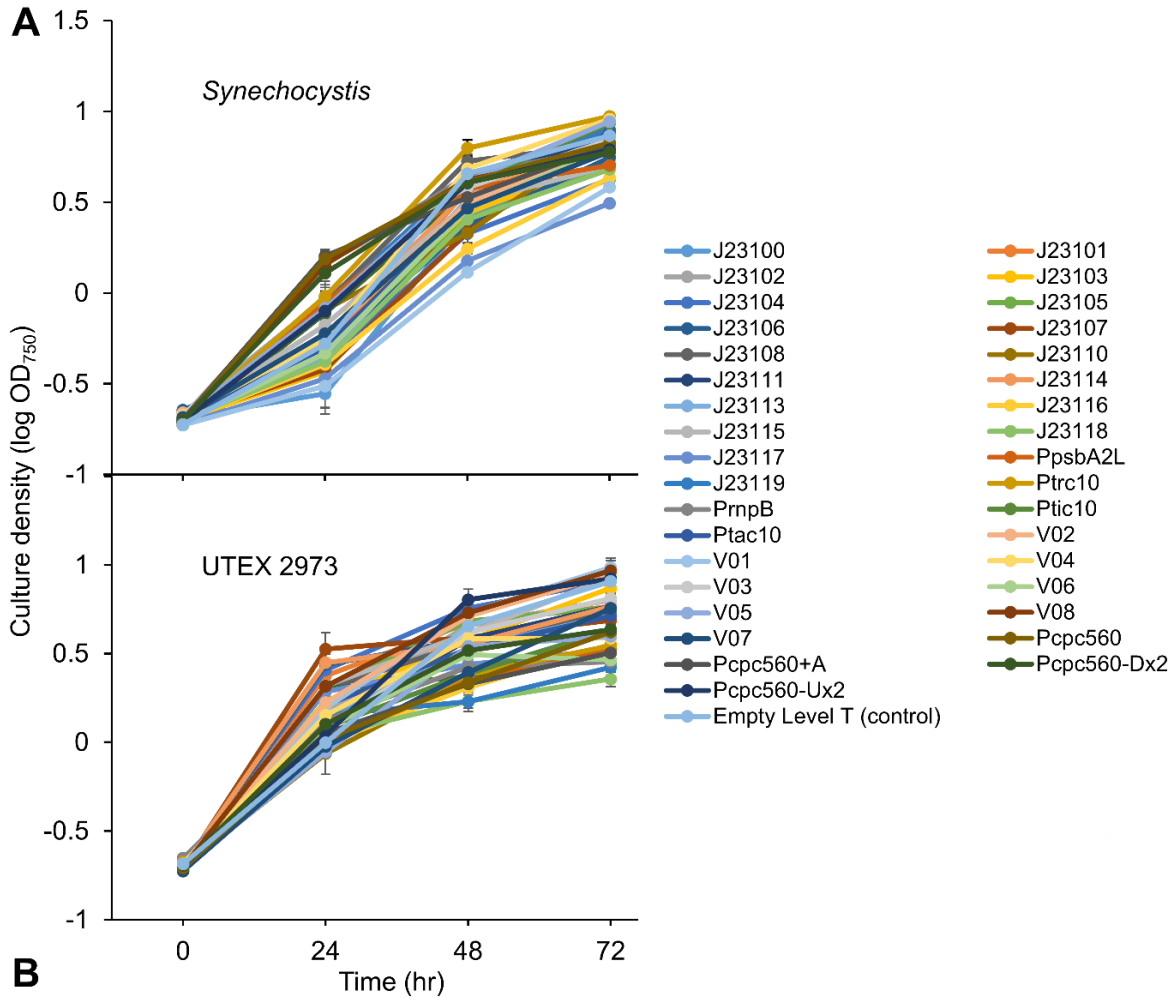
The screenshot displays the DAB tool interface. At the top, a navigation bar includes the 'dab' logo, a 'Design assemblies' link (marked with a red circle '1'), 'Manage parts', 'About', and a user login 'Logged as standard\_parts' with a 'Log out' link. The main heading is 'Design assemblies'. On the left, a sidebar titled '+ Add a construct' lists various templates: EMMA, MoClo, Phytobricks-L1, MoCloPlant-L1, and Cyanogate. Under Cyanogate, three options are listed: L1-knockin, L1-knockout, and L1-standard (marked with a red circle '2'). Below this are options for 'Upload constructs', 'Export project', and download links for 'JSON (for later use)', 'Genbank (final sequences)', and 'PDF schemas'. At the bottom of the sidebar is an 'Order' button (marked with a red circle '3'). The main content area shows a 'Cyanogate project' with two assembly options: 'Standard' and 'Knockout'. The 'Standard' option is selected and shows a schematic with components: BACKBONE, TSS, RBS, SP, CDS2-STOP, and 3U+TER. The 'Knockout' option shows a schematic with components: BACKBONE, UP, sacB, ABR, and DOWN.

**Supplementary Figure S1. Comparison of growth for *Synechocystis*, PCC 7942 and UTEX 2973 under different culturing conditions.** Values are the means  $\pm$  SE from at least five biological replicates from two independent experiments.



**Supplementary Figure S2. Growth and expression levels of heterologous and synthetic promoters in *Synechocystis* and UTEX 2973.** (A) *Synechocystis* and UTEX 2973 was cultured for 72 hr at 30°C with continuous light ( $100 \mu\text{mol photons m}^{-2} \text{s}^{-1}$ ) and 40°C with  $300 \mu\text{mol photons m}^{-2} \text{s}^{-1}$ , respectively (see **Fig 6**). Expression levels of eYFP are shown at three time points (24, 48 and 72 hr after inoculation). Values are the means  $\pm$  SE from at least four biological replicates where each replicate represents the median measurements of 10,000 cells.

**A Golden Gate-based toolkit for engineering cyanobacteria**



**Supplementary Figure S3. Cell volume calculations for *Synechocystis* and UTEX 2973 from confocal microscopy images.** (A) Example confocal images of *Synechocystis* (left) and UTEX 2973 (right) cells expressing eYFP driven by the J23119 promoter at 48 hr. Individual cells were selected and measured using Leica AF Lite software (Leica Microsystems). Top panel: eYFP fluorescence (green); middle panel: chlorophyll autofluorescence (red); bottom panel: overlay of eYFP and chlorophyll signals (yellow). (B) Volume estimations based on confocal image data (n =50) (C) Mathematical formulas used for calculating cell volume based on the cell shapes of *Synechocystis* (coccus, spherical) and UTEX 2973 (bacillus, cylindrical).

